FORCES ON A VERTICAL CIRCULAR CYLINDER DUE TO REGULAR AND RANDOM WAVES

A Thesis Submitted

in Partial Fulfilment of the Requirements

for the Degree of

MASTER OF TECHNOLOGY

by

BIJAY KUMAR PANDAY

to the

DEPARTMENT OF CIVIL ENGINEERING

INDIAN INSTITUTE OF TECHNOLOGY KANPUR

DECEMBER 1994

CE-1994-M-PAN-FOR

CERTIFICATE

It is certified that the work contained in this thesis entitled " **FORCES ON A VERTICAL CIRCULAR CYLINDER DUE TO REGULAR AND RANDOM WAVES** ", by " **BIJAY KUMAR PANDAY** ", has been carried out under our supervision and that this work has not been submitted elsewhere for a degree.

S. Surya Rao

Dr S. SURYA RAO
PROFESSOR
DEPTT. OF CIVIL ENGG.
I.I.T. KANPUR

K Muralidhar

Dr K. MURLIDHAR
ASSOCIATE PROFESSOR
DEPTT. OF MECH. ENGG.
I.I.T. KANPUR

DECEMBER , 1994

ABSTRACT

The present work is a practical approach to study the nature of forces arising from one-dimensional sea-waves. The waves, both regular and random were generated by a wavemaker in a wave flume. The wavemaker is PC-controlled. Forces and moments acting on the vertical cylinder installed in the flume were measured by two properly mounted force transducers. The cylinder was vertically mounted as a cantilever with no support at the bottom.

Both in-line and transverse forces acting on the cylinder have been measured. The transverse forces are generally less than in-line forces in case of bottom-supported structures. However, in the present study, the dynamic response of the cylinder and its vibrations due to the free end at the bottom is seen to result in higher values of transverse forces compared to in-line forces. Experimentally determined forces and moments have been compared with the forces and moments predicted by the Morison equation.

Experimental results for regular waves are seen to match with results of linear theory. For random waves, water surface elevation, forces and moments have been recorded. Data has been analysed using Fast Fourier transform alogrithm to get wave, force and moment spectra. The theoretical spectra have also been computed using a linearisation of Morison equation. Experimental force and moment spectra are seen to follow the same trend as the theoretical spectra over a limited range of frequencies.

ACKNOWLEDGEMENT

The author would like to express his deep sense of gratitude to his thesis advisors Dr. S. Surya Rao and Dr. K. Muralidhar for their valuable guidance, inspiration and encouragement during the course of this work.

Special thanks are being extended to Dr. B. S. Murthy, Dr. B. Dutta, Dr. K. Subramanya, Dr. S. Ramaseshan and Dr. S.Surya Rao of the department of Civil Engineering for thought-provoking guidance, they have provided to the author.

There are many people to thank for aiding in this effort. The kind gesture and cooperation during the whole experimental work given by Sri Suresh Kumar, Sri Kalyan Das, Sri Ramshankar, Sri J. C. Gupta and Sri Sitaram, all of Hydraulics Laboratory can never be forgotten.

Finally, the author would like to acknowledge all his friend specially Apurb, Anup Singh, Bhuwaneshji, Dixitji, Jhaji, Mishraji Naidu, Wasan, Thakur , Sonkar,Srivastava, Tamatar and others fo their consistent encouragement given by them during the who M.Tech programme.

TABLE OF CONTENTS

LIST OF FIGURES

LIST OF PHOTOGRAPHS

LIST OF TABLES

LIST OF SYMBOLS

The following symbols have been used in this thesis

C_d = drag coefficient

C_m = inertia coefficient

c_G = group velocity of wave

c = wave celerity

D = diameter of cylinder

d = depth fo still water

F_i = inertia force

F_d = drag force

f = frequency

f_o = peak frequency

g = gravitaional acceleration

H_s = significant waveheight

H = waveheight

K = wave number

K' = Keulegan-Carpenter number

k' = roughness

K_d = drag constant

K_i = inertia constant

m = mass

Re = Reynolds number

S = spectral density

T = time period

t = time

U_m = maximum surface velocity

U = velocity of fluid

z = elevation

ω = angular frequency

θ = directional parameter

σ^2 = variance

ρ = density

ν = kinematic viscosity

ϵ = spectral width parameter

CHAPTER I

Introduction

The waves generated at the surface of seas induce forces on the structures installed in them. It is of utmost interest for a structural designer to know the dynamic characteristics of the wave loading.

The present work is a simple approach for studying the wave characteristics and the corresponding force and moment characteristics. The model is simplified in the sense that only one dimensional waves have been studied. The waves are generated in a wave flume by a wavemaker. Studies have been carried out with regular waves and random waves with Jonswap spectra. Theoretical and experimental force and moment spectra have been obtained and compared.

In the present thesis, Chaper 2 deals with the literature review and the proposed theories available for regular as well as random waves. Chapter 3 deals with the experimental details and the procedure adopted for conducting experiments. Results have been presented in Chapter 4 and have been subsequently discussed. Chapter 5 presents conclusions of the present work. Appendix A contains computer programs written in Fortran 77 and the sea-language software for running the PC-controlled wavemaker. Appendix B deals with the calculations for regular waves. Some relevant definitions have been included in Appendix C.

CHAPTER II

Literature Review

2.1 Background Study

Sea-waves can induce both in-line and transverse forces on an offshore structure. The lift forces are induced due to vortex shedding. The fundamental results of interest concern the inertia force, which is exerted on a body held in a uniformly accelerating ideal fluid and the drag force arising from an asymmetric distribution of pressure. The inertia force is written as,

$$F_i = C_m \rho V \frac{du}{dt} \qquad (2.1)$$

where,

F_i = inertia force

C_m = inertia coefficient

ρ = density of fluid

V = volume of body

$\frac{du}{dt}$ = acceleration of fluid

A method of calculating wave forces on piles was first proposed by Morison, Johnson, O'Brien and Schaaf (1950) and this provided a landmark in wave force prediction methods. Morison and his co-workers suggested that the forces acting on a section of a pile due to wave motion is made of two components: a drag force, analogous to the drag on a body subjected to steady flow of a real fluid associated with wake formation behind the body; and an inertia force, analogous to that on a body subjected to a uniformly accelerated flow of an ideal fluid.

Morison equation is thus expressed as follows:

$$F = 0.5 \rho D C_d U|U| + 0.25 \rho \pi D^2 C_m \frac{dU}{dt} \qquad (2.2)$$

where,

D = diameter of cylinder

U = incident (undisturbed) velocity taken at the section centre

C_d = drag coefficient

C_m = inertia coefficient

The application of Morison equation carries the implicit assumption that the body size is small relative to the wavelength so that the incident flow is virtually uniform in the vicinity of the body. When the body size is large, this equation is no longer valid.

Hydrodynamic coefficients for forces on a circular cylindrical structure have received considerable attention. A systematic approach in this direction was made by Keulegan and Carpenter (1958) who tested horizontal tubes at the node of a standing wave in a tank so that the tubes essentially experienced one dimensional flow. It was observed that C_d and C_m depend on a period parameter known as Keulegan-Carpenter number defined as $\frac{U_m T}{D}$, where U_m is the maximum water particle velocity, T = the time period and D = diameter of the cylinder

Relatively recent is the finding of Sarpkaya (1976). In his study, tests were conducted on horizontal cylinder in a vertical U-tube in which water was harmonically oscillated. He also found C_d and C_m to be dependent on the time period.

Sarpkaya (1974) and Tutor (1974) have measured the lift (transverse) forces on their test cylinders. They found the

presence of several lift frequencies in a given wave cycle. A dominant frequency of vortex-shedding was shown to exist at twice the wave frequency. When C_L was plotted against $\frac{U_m T}{D}$, the maximum lift force was observed to be as high as 1.3 times the maximum in-line drag force.

Flexible oscillating cylinders have been studied by Laird (1962). It was found that dynamic response of the body could lead to high lift, as high as 4.5 times the drag on a fixed cylinder in an uniform flow. Thus the degree of rigidity and support conditions of the structure control significantly the lift characteristics.

Isaacson (1974) observed that for $\frac{U_m T}{D} < 2$, the flow did not separate. For $\frac{U_m T}{D} \simeq 4$, a pair of eddies formed, which attached to the cylinder and moved symmetrically back and forth during each half cycle of wave. For $\frac{U_m T}{D}$ in the range 6-15, one eddy separated completely during each half cycle. Isaacson calculated the first five components of the lift coefficients. These were written as a function of the Keulegan-Carpenter number $\left(\frac{U_m T}{D} \right)$.

These findings gave impetus to research in wave mechanics and form the main background for the present work.

2.2 Aim of Study

The aim of the present study is to measure the wave forces for the case of regular and random waves and to examine whether these forces can be predicted.

2.2.1 Regular waves

When a cylinder is subjected to one dimensional regular

waves of various frequencies and small waveheights, it experiences inline and transverse (lift) forces. Maximum in-line force and moment can be theoretically predicted using the following important variables:

$\frac{H}{gT^2}$ = dimensionless wave steepness

$\frac{d}{gT^2}$ = dimensionless still water depth

$\frac{k'}{D}$ = relative pile roughness

$\frac{HD}{T\nu}$ = a form of Reynolds Number.

A appropriate wave theory is assumed to determine the theoretical value of the hydrodynamic coefficients C_d and C_m. From the calculations presented by Dean (1965a), curves have been prepared in the form of isolines for various $\frac{C_m D}{C_d H}$ ratios. These plots are available in the form of wave steepness as a function of the dimensionless depth $\frac{d}{gT^2}$. Thus one can get theoretical maximum in-line forces and moments acting on the circular cylinder subjected to a unidirectional regular wave.

Sarpkaya (1976b, 1977a) has measured the transverse forces acting on smooth and sand-roughened cylinders for a wide range of Reynold numbers, Keulegan-Carpenter numbers and relative roughnesses. These results are available in graphical form. They have been used for comparison in the present work.

2.2.2 Wave forces due to Random Waves

Ocean waves are random in nature. Thus getting statistical characteristics of random waves is of concern in ocean engineering. Random waves result in random loads on offshore

structures. A random wave can be decomposed into several regular waves each of unique amplitude and frequency.

In the present thesis, random (Jonswap) wave spectra have been dealt with and the consequent loading namely, force and moment spectra have been determined.

Before going into details of spectral analysis, it is worthwhile to discuss some of the statistical properties of random waves. These are given below

$$\text{Variance, } \sigma_x^2 = \int S_x(f)\, df$$

where $S_x(f)$ is a continuous function of frequency. $S_x(f)$ represents the contribution to variance (or "energy") of signal $x(t)$ due to its content within the frequency range f to f + df. Symbolically we can write as

$$S_x(f)\, df = \sum_{f_n}^{f_n+df} \frac{1}{2} |A_n|^2 \qquad (2.3)$$

where random wave signal can be expressed in a Fouries series as follows

$$x(t) = Re \left\{ \sum_{n=1}^{\infty} A_n\, e^{-2\pi n f_o t} \right\} \qquad (2.4)$$

After the signal is recorded we can easily get the spectra using Fast Fourier transform (FFT) alogrithm.

Similar spectra can also be derived for the force and moment signals recorded in the experiments.

One more important characteristic of random waves is H_s, the significant wave height. It is a value above which $\frac{1}{3}$ of the largest wave components are present.

In order to find the nature of the probability distribution for the wave heights, we define a spectral width parmeter

$$\epsilon = \left(1 - \frac{m_2^2}{m_o m_4}\right)^{1/2} \qquad (2.5)$$

where $m_o = \int_o^\infty S_x(f).\, df$

$m_2 = \int_o^\infty f^2 . S_x(f)\, df$

$m_4 = \int_o^\infty f^4 . S_x(f)\, df$

A value of $\epsilon = 1.0$ indicates Gaussian Distribution and $\epsilon = 0.0$ indicates Rayleigh Distribution.

2.2.3 Alternative approach to represent one dimensional spactra

The free surface elevation can be written in general as follows

$$\eta = \sum_{n=1}^{\infty} A_n \exp\left\{i\left[K_n \cos(\theta_n)x + K_n \sin(\theta_n)y - 2\pi f_n t\right]\right\} \qquad (2.6)$$

where A_n = complex amplitude.

Generalised three dimensional spectrum can be written as $S(K,f,\theta)$; such that $S(K,f,\theta)dK.df.d\theta$ represents the contribution to the variance σ_n^2 due to component waves with wave numbers between K and K+dK, frequencies between f and f + df and directions between θ and $\theta + d\theta$.

Thus we have

$$S(K,f,\theta)\, dK\, df\, d\theta = \sum_{K_n}^{K_n+dK} \sum_{f_n}^{f_n+df} \sum_{\theta_n}^{\theta_n+d\theta} \frac{1}{2} |A_n|^2$$

VAriance $\sigma_n^2 = \int_o^\infty \int_o^\infty \int_{-\pi}^{\pi} S(K,f,\theta)\, dK\, df\, d\theta \qquad (2.7)$

This general three dimensional spectrum is too unwieldy for practical use. So, in two dimensions it can be written as

follows

$$\sigma_n^2 = \int_0^{\infty} \int_{-\pi}^{\pi} S(f,\theta)\, df\, d\theta \qquad (2.8)$$

where the two dimensional directional frequency spectrum $S(f,\theta)$ can be obtained from the following numerical integration

$$S(f,\theta) = \int_0^{\infty} S(K,f,\theta)\, dK \qquad (2.9)$$

The directional frequency spectrum $S(f,\theta)$ has found general application in engineering. Similarly, other spectra such as directional wave number spectrum $S(K,\theta)$ can also be obtained.

Now from these two dimensional spectra, one dimensional wavenumber and frequency spectra may be obtained by integrating the corresponding directional spectra over θ, giving

$$S(f) = \int_{-\pi}^{\pi} S(f,\theta)\, d\theta \qquad (2.10)$$

$$S(K) = \int_{-\pi}^{\pi} S(K,\theta)\, d\theta \qquad (2.11)$$

and the variance σ_n^2 is given as

$$\sigma_n^2 = \int_0^{\infty} S(f)\, df = \int_0^{\infty} S(K).dK$$

The relationship between the directional wavenumber and frequency spectra is given as

$$S(K,\theta) = \frac{1}{2\pi} C_G\, S(f,\theta) \qquad (2.12)$$

where

C_G = group velocity

$$= \frac{d\omega}{dK} = 2\pi \left[\frac{df}{dK} \right]$$

Transformation of random wave train due to refraction was described originally by Longuet-Higgins (1956, 1957b). It has

been shown that the energy flux between neighbouring orthogonals of any component wave train remains constant. Hence,

$$S(f,\theta)\, df\, d\theta\, C_G b = S_o(f_o,\theta_o)\, df_o\, d\theta_o\, C_{G_o} b_o \qquad (2.13)$$

This is equivalent to assuming linearity and hence no energy transfer between any pair of frequencies. It can also be shown that

$$bK\, d\theta = b_o K_o d\theta_o = \text{constant} \qquad (2.14)$$

Substituting Equation (2.14) into Equation (2.13) and bearing in mind that $\frac{K}{K_o} = \frac{C_o}{C}$ (since f is constant), we obtain

$$C\, C_G\, S(f,\theta) = C_o\, C_{G_o}\, S_o(f, \theta_o)$$

$$= \text{Constant along an orthogonal.}$$

In the present work random waves have been generated using Jonswap spectra with a randomized initial phase. The Jonswap spectrum is basically a modification of the Pierson-Moskowitz spectrum (1964). The Pierson-Moskowitz spectrum can be written as

$$S(f) = \frac{\alpha g^2}{(2\pi)^4 f^5} \exp\left[\frac{-\beta}{f^4}\right] \qquad (2.15)$$

where α and β are constants and f is frequency. The constant β depends on velocity U, and is valid for a fully developed condition.

The Jonswap spectrum accounts for fetch-restrictions and provides a much sharper peaked spectrum. Jonswap spectrum is given as

$$S(f) = \frac{\alpha g^2}{(2\pi)^4 f^5} \exp\left[\frac{-5}{4}\left(\frac{f}{f_o}\right)^{-4}\right] \gamma^a \qquad (2.16)$$

where $a = \exp\left[1 - (f-f_o)^2/2\sigma^2 f_o^2\right]$

$$\sigma = \begin{cases} \sigma_a = 0.07 & \text{for } f \leq f_o \\ \sigma_b = 0.09 & \text{for } f > f_o \end{cases}$$

Here, f_o is the peak frequency at which S(f) is maximum and γ is ratio of maximum spectral density in the Jonswap spectrum to the maximum spectral density in the Pierson-Moskowitz spectrum.

Based on these spectra, we are in a position to discuss the theoretical spectra of random wave forces.

2.2.4 Random wave forces

So far we have discussed the statistical nature of waves themselves. We turn now to consider the consequent loading on a structural element. The basic assumption here is that the Morison Equation (2.2) is always valid. Therefore a statistical description of fluid velocities and accelerations is required.

Using linear theory, velocity and acceleration of wave trains are given as

$$\left.\begin{aligned} U(t) &= H_u(f)\,\eta(t) \\ a(t) &= H_a(f)\,\eta(t) \end{aligned}\right] \qquad (2.17)$$

where $\eta(t)$ is the input wave height signal. Further,

$$H_u(f) = 2\pi f \frac{\text{Cos h } (K(Z+d)}{\text{Sin h } (Kd)}$$

$$H_a(f) = -i4\pi^2 f \frac{\text{Cos h } (K(Z+d)}{\text{Sin h } (Kd)}$$

Consequently the corresponding velocity and acceleration spectra are given as

$$\left.\begin{aligned} S_u(f) &= |H_u(f)|^2 \; S_\eta(f) \\ S_a(f) &= |H_a(f)|^2 \; S_\eta(f) \end{aligned}\right] \qquad (2.18)$$

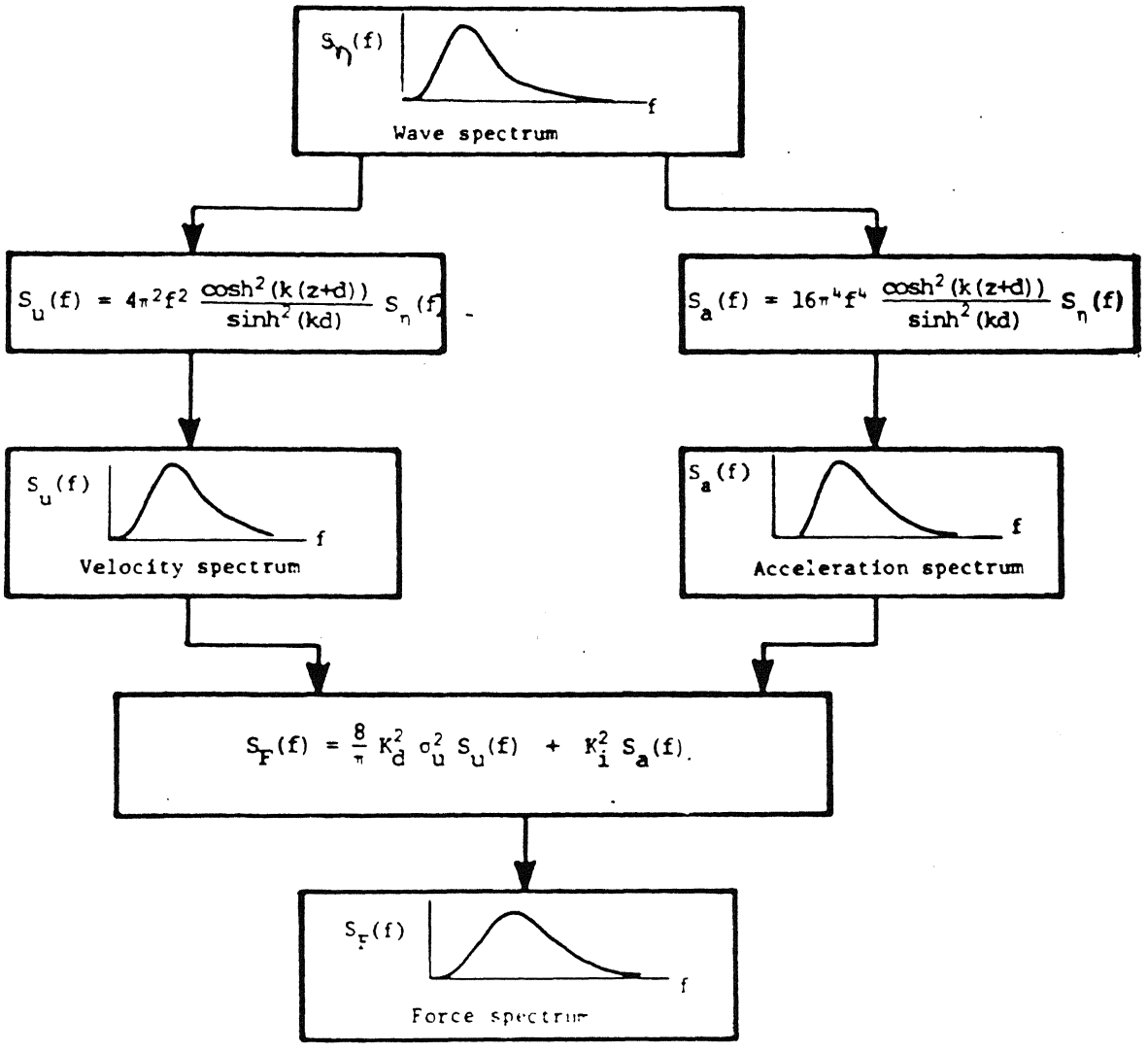

Fig.2.1 Flow Chart to Calculate Velocity Spectrum, Acceleration Spectrum and Force Spectrum

Now from the above probabilistic properties of velocity and acceleration spectra, Morison equation gives the statistical model of force as follows

$$F(t) = K_d\, u(t)\, |u(t)| + K_i\, a(t) \qquad (2.19)$$

Coefficients K_d and K_i are drag and inertia terms respectively and are assumed as constant for the whole depth of the cylinder. Here,

$$K_d = \frac{1}{2} \rho D\, C_d$$

$$K_i = \rho \left[\frac{\pi D^2}{4} \right] C_m$$

and ρ, D, C_d and C_m are density of fluid, diameter of cylinder, drag coefficient and inertia coefficient, respectively.

The spectral density of forces can now be found using the flow chart given in Figure 2.1.

In the figure given above, $S_F(f)$ is the spectral density of predicted force on a section of the cylinder. Parameter σ_u^2 is the area of the velocity spectrum at a fixed elevation Z.

In the present thesis total force acting on the cylinder has been measured. The experimental force spectra hence correspond to the total force spectra.

In order to get the theoretical spectrum for the full cylinder the above predicted sectional force spectra given in Figure 2.1 should be integrated numerically over the entire depth of immersion.

Borgman (1967,b) has provided force as well as the moment spectra for a single cylinder extending from the sea-bed and piercing the free surface. They are as follows

$$S_{FT}(f) = S_{\eta}(f)\left\{ \frac{8}{\pi} \left[\frac{2\pi f K_d}{\text{Sin h}(Kd)} \int_{-d}^{o} \sigma_u(Z)\ \text{Cosh}\,(K(Z+d))dZ \right]^2 + \frac{(2\pi f)^4\ K_i^{\,2}}{K^2} \right\} \qquad (2.20)$$

$$S_{MT}(f) = S_{\eta}(f)\left\{ \frac{8}{\pi} \left[\frac{2\pi f K_d}{\text{Sin h}(Kd)} \int_{-d}^{o} (Z+d)\sigma_u(Z)\ \text{Cosh}(K(Z+d))dZ \right]^2 + \left[\frac{(2\pi f)^2 K_i[\,(Kd)\ \text{Sinh}(Kd) + 1 - \text{Cosh}(Kd)\,]}{K^2\ \text{Sinh}\,(Kd)} \right]^2 \right\} \qquad (2.21)$$

Here $S_{\eta}(f)$ is the known experimental wave spectrum. $S_{FT}(f)$ and $S_{MT}(f)$ are the total force and moment spectra. $\sigma_u(z)$ can be derived from the predicted velocity spectra at each section of the cylinder. Other constants and variables have been defined earlier.

The goal of the present work is to derive the theoretical spectra for total force and moment using Equations (2.20) and (2.21) and to compare them with the experimentally measured profiles.

CHAPTER III

EXPERIMENTAL DETAILS

3.1 Equipment

Experiments were conducted in a wave flume having 24m length, 45 cm width and 90 cm depth and having glass walls on the two sides. All experiments were conducted at a still water depth of 70 cm. The wavemaker consisting of control box, interface box and wavegauge was installed at the upstream end of the flume so that waves could be generated at the desired parameters set appropriately. An aluminium cylinder of 5 cm diameter was fabricated and installed in the flume as shown in the Figure 3.1. It was fitted with two transducers vertically separated by a distance of 5 cm. The idea behind putting two transducers is to measure forces as well as moments simultaneously. A well supported top end also facilitates supporting the cylinder in the experiment. The wavemaker and the cylinder in mounted position can be seen in photographs Nos. 1 to 5.

The measurements were taken for a given wave signal input forces in longitudinal (in-line force) and transverse (lift force) directions.

3.2 Instrumentation

The experimental setup to determine the wave characteristics is shown in Figure 3.1 and Figure 3.2. The instrumentation consists of wavegauge, control box, wavemaker, two force transducers, interface box and oscilloscope. Their specifications have been presented in Section 3.4.

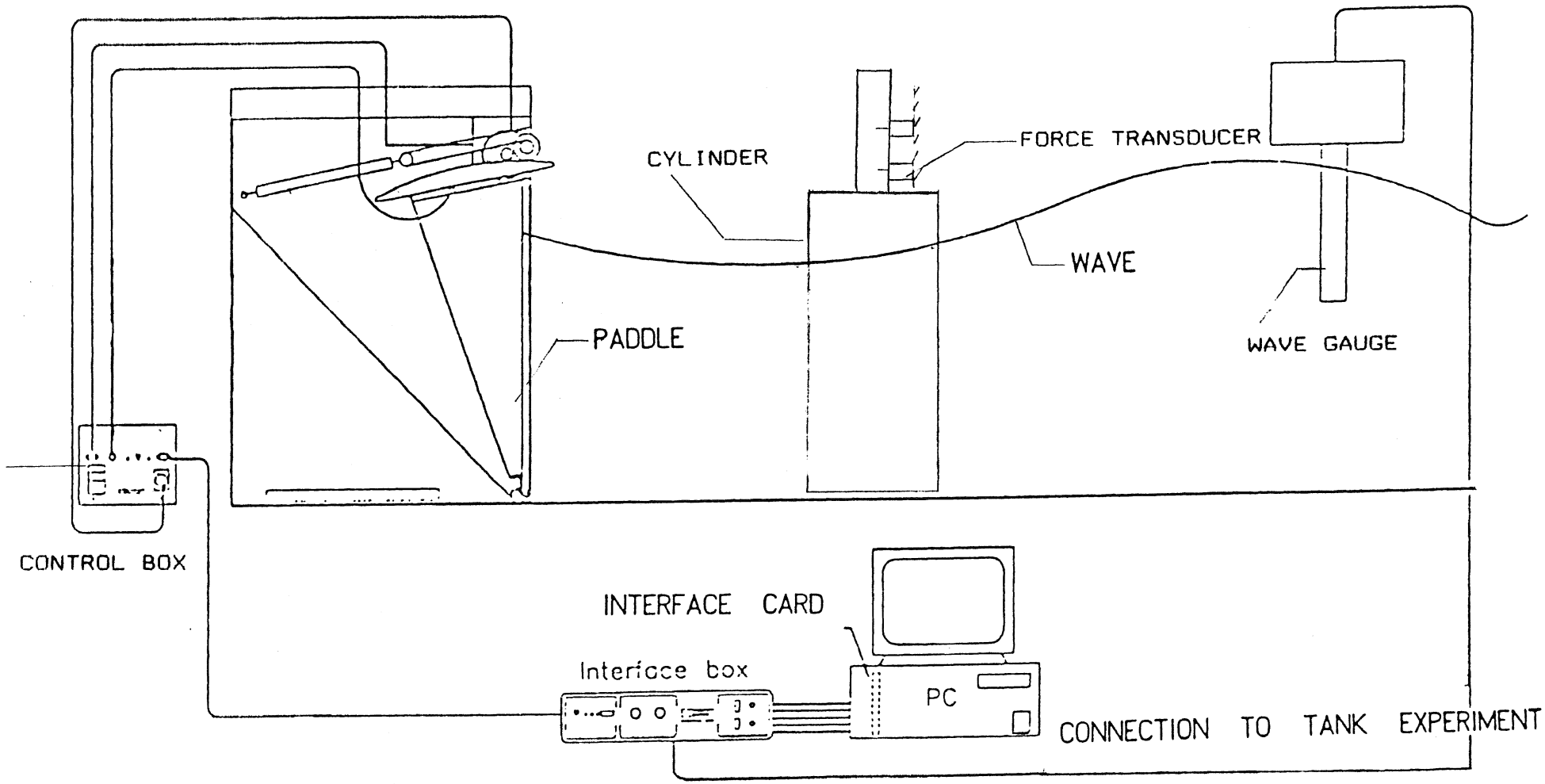

Fig.3.1 A Schematic Illustration of Wavemaker and Instrumentation

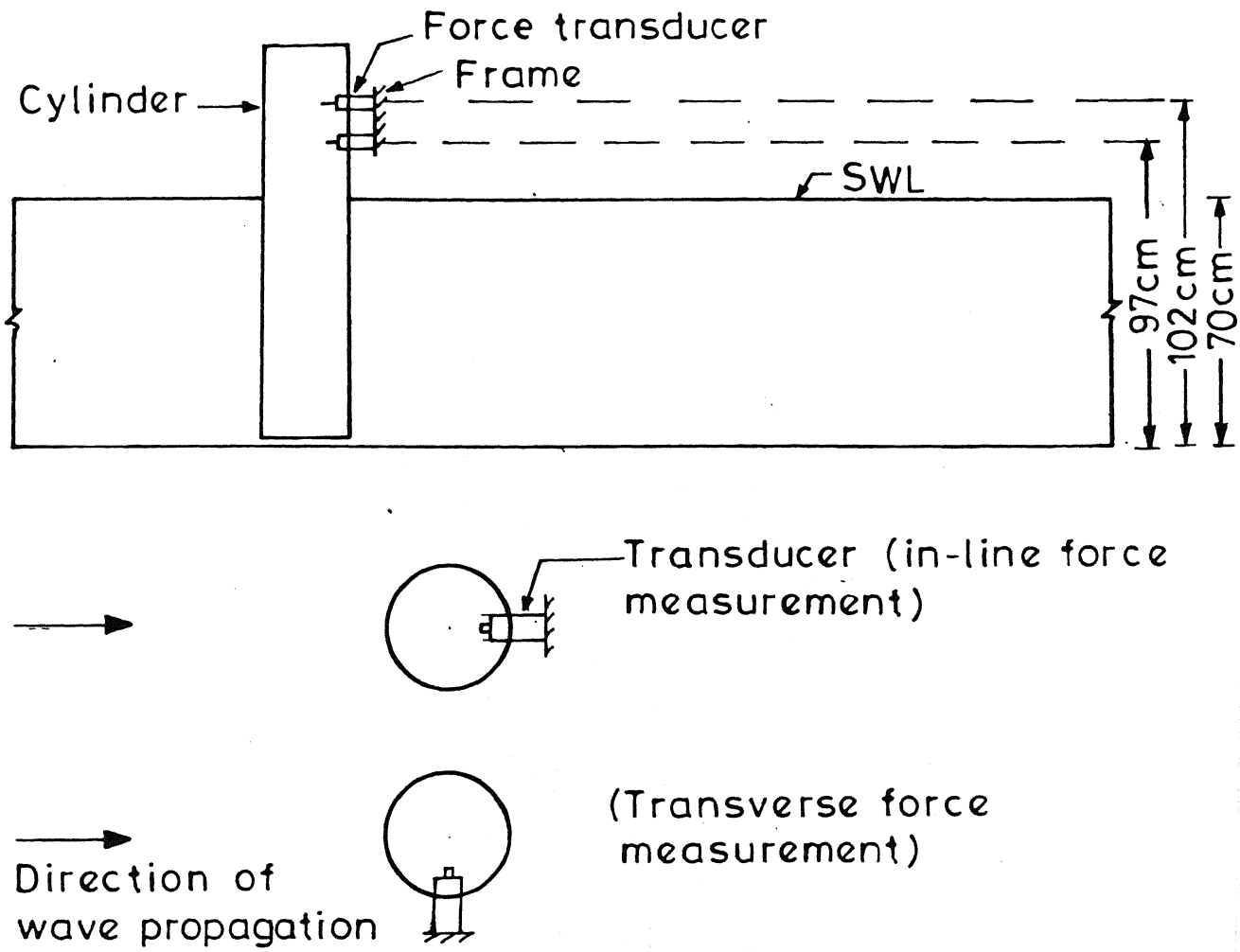

FIG.3.2 LONGITUDINAL SECTION OF THE CHANNEL AND PLAN VIEW OF THE CYLINDER INSTALLED (Dimensions are not to the scale)

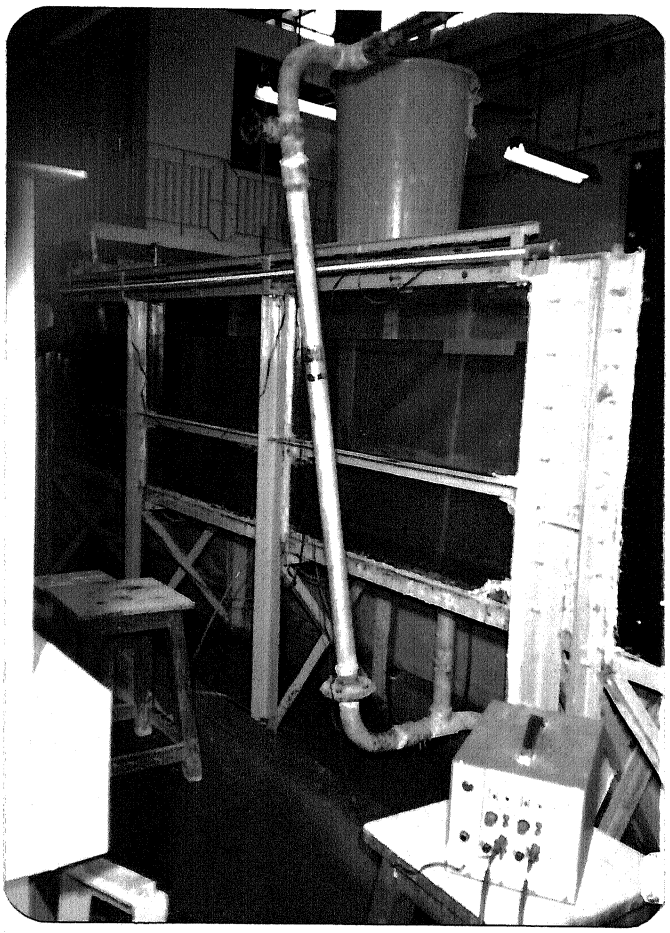

Photo. 1 Photograph showing the wave flume with piping for filling and emptying the wave flume and wave monitor

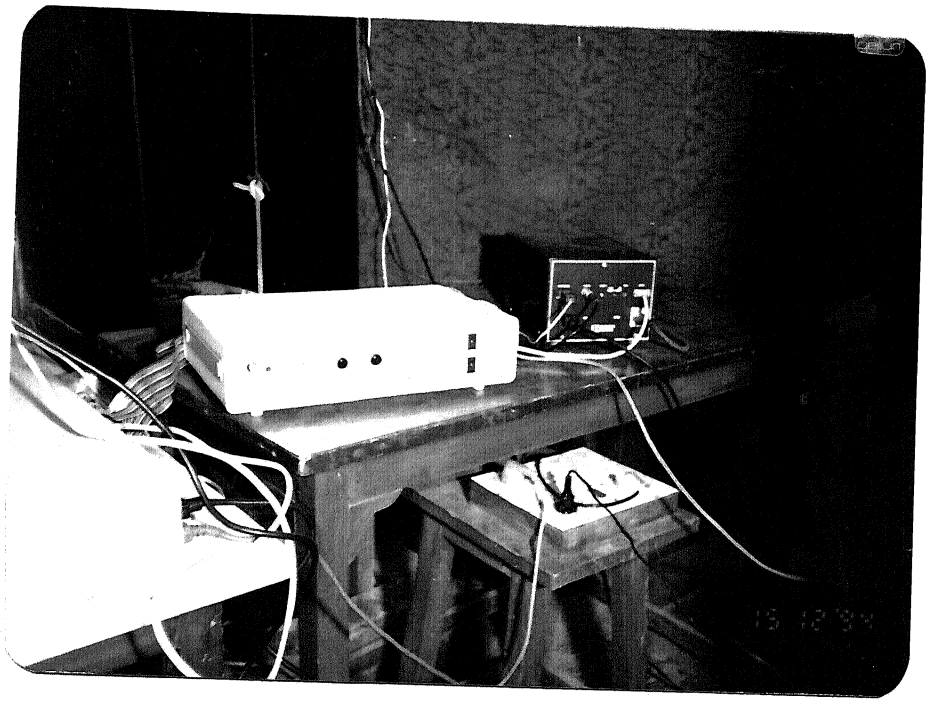

Photo. 2 Photograph showing the interface box and control box

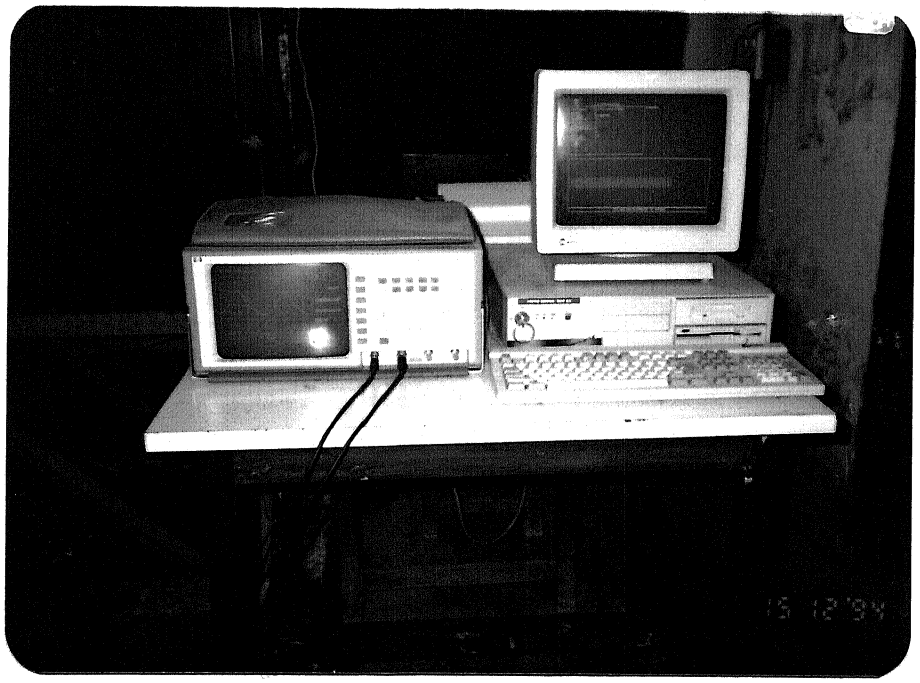

Photo. 3 Photograph showing the storage oscilloscope and PC

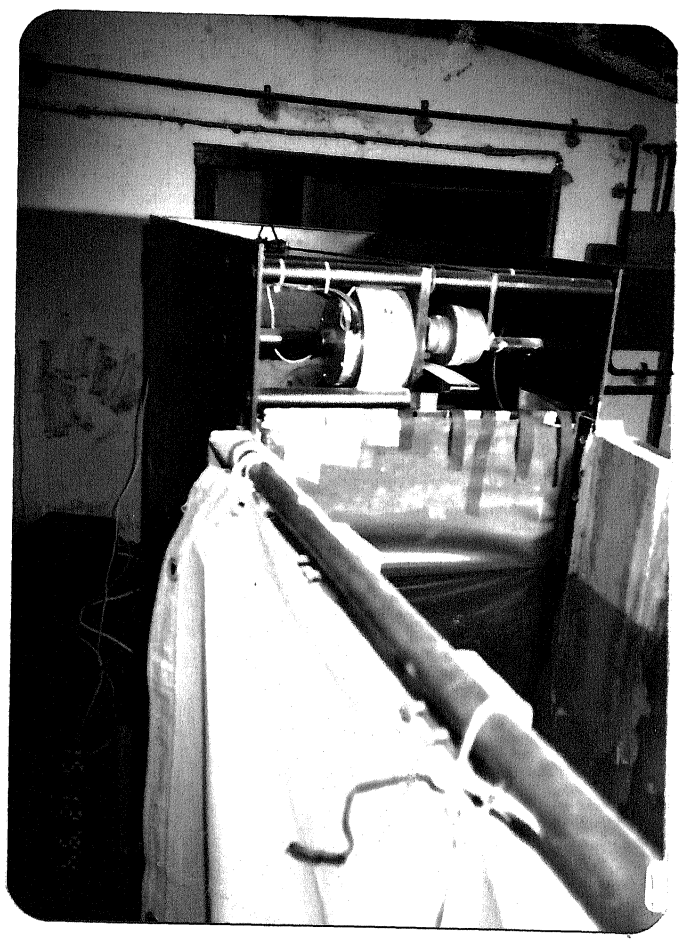

Photo. 4 Photograph showing the wavemaker

Photo. 5 Photograph showing the cylinder mounted in position with the force transducers, channel selector, conditioning amplifier and wave probe

A wavegauge is used to measure the water surface elevation (η) at any instant (t). It is of capacitance type and is linear in the working range with a ± 10 volt output. In order to convert the data obtained (in volts) to cm units, the wavegauge is calibrated using an oscilloscope.

The control box contains the power amplifier for the wavemaker, along with signal conditioning, force feedback, wave absorption and nonlinearity correction circuitry.

The wavemaker consists of a 'flap' which is a wedge shaped paddle pivoted about its tapered end on a fabric hinge fixed to the bottom leading edge of the wavemaker box. The paddle is mounted in the box and extends the full width of the tank. The front of the box is sealed with a waterproof fabric gusset, behind which the paddle moves. The paddle is driven by an electric servo-motor via a berrillium-copper drive belt which runs over a sector attached to the top of paddle.

The two force transducers are of model 8200 (Bruel and Kjaer, Denmark) and sense forces in the range (-1000 N to 5000 N). Their specifications have been given in section 3.4.

The interface box acts as the junction between the wavemaker and the outside world. All the signals to and fro the interface card in the back of PC are run by ribbon cable to the interface box. The box also contains a sine wave generator for running the wavemaker without using the PC. The system is run from an internal power supply.

The interface card is manufactured Advantech (Model PCL 812) and plugs into the expansion slot of any IBM-compatible PC. It provides two 12 bit analogue output channels, 16 analogue

inputs, 16 digital inputs and 16 digital outputs.

The instrumentation can be seen in photographs Nos. 1 to 5.

3.3 Procedure

The 5 cm diameter aluminium cylinder of height 90 cm was installed in the flume as shown in the Fig. 3.2. The cylinder was connected to the force transducers (8200 type) in the in-line as well as transverse directions in separate experiments to measure in-line forces and lift forces, respectively.

The wavemaker operates for 1.5 minutes for each run. Data are recorded at 0.0625 seconds intervals.

For regular waves of required amplitude and frequency, the wavemaker was run with suitable software through a PC. The data output (wave gauge signal and force signal) were recorded simultaneously. A given input signal was run twice to get the in-line and transverse (lift) forces.

Similarly, for random waves the wavemaker was run to produce a Jonswap spectrum. All time-based signals were analysed using the Fast Fourier transform alogrithm; a computer program for this alogrithm is given in the Appendix A.

For force signal analysis, the transducers were connected to the conditioning amplifier for amplification of signals and conditioning amplifier was connected directly to the Interface card to store the data.

A total of eleven experiments have been conducted in the flume. Out of these, six are for regular waves at different amplitudes and frequencies, and five experiments have been

conducted for Jonswap spectra, set at five different peak frequencies. The parameters for the different experiments are tabulated in Tables 1 and 2 for regular and random waves, respectively.

The results have been produced in tabular as well as in graphical form.

3.4 Specifications

3.4.1 Oscilloscope

Model number	:	HP 54501 A Diziting Oscilloscope
Manufacturer	:	Hewlwett Packard
No. of input channels	:	4
Input coupling	:	AC, DC
Vertical sensitivity	:	Maximum 5V/div Minimum 5mV/div
Vertical gain accuracy (dc)	:	+ 1.5%
Time base accuracy	:	0.005%
Time base range	:	2 ns/dv to 5 s/div
Maximum sampling rate	:	10 MSa/s

3.4.2 Conditioning amplifier

Model	:	Type 2626
Manufacturer	:	Bruel and Kjaer, Denmark
Maximum sensitivity	:	1000 mV/PC
Output modes	:	Direct and transformer coupled.
Frequency limits	:	Switchable low and high frequency.

Calibrated output rating	:	0.001-10 V/unit selectable in 20 dB steps.
Maximum output	:	10 V (10 mA) peak from 0.3 Hz to 30 KHz.
Level indicator	:	"overload" Led lights when input or output levels exceed 10V peak.
Rise time	:	~ 2.5 V/μS
Recovery time	:	< 200 μS
Environmental condition	:	
Temperature range	:	-10 to + 55°C
Humidity	:	0 to 90% RH
Power requirements	:	100-240V (50-400 Hz) ± 10% AC.7VA complies with safety class 1 of EC 348.

3.4.3 Force Transducer

Type	:	B & K Type 8200
Manufacturer	:	Bruel & Kjaer, Denmark
Force range	:	1 KN tensile to 5 KN compressive.
Linearity	:	< ± 1% of maximum force
Charge sensitivity	:	4.0 PC/N
Sliffness	:	5.0×10^9 N/m
Weight	:	21 gram

3.4.4 PC

Type	:	386 SX
Manufacturer	:	Wipro (Pvt) Ltd., Bangalore

3.4.5 Interface Card

Model	:	PCL 812
Digitisation	:	12 bit
No. of channels	:	16 A/D
Maximum sampling rate	:	5 KHz

3.4.6 Wavegauge

Type	:	Capacitance
Output voltage	:	± 10 volts.
Manufacturer	:	Armfield, U.K.

CHAPTER IV

RESULTS AND DISCUSSIONS

The results have been presented in tabular form in Tables 1-9, and as graphical plots in Figures 4.1 - 4.8 at the end of the chapter.

Regular waves -

In order to calculate the drag coefficient (Cd), the inertia coefficient (C_m) and the lift coefficient (C_L), Reynolds number and Keulegan-Carpenter number for each experiment are required. These are listed in Table 3. Table 4 shows the comparison between maximum in-line force and maximum in-line moment measured and those predicted by theory. Sample calculation for determining the maximum in-line force and moment are given in Appendix B. Table 5 shows a comparison between the lift force found experimentally and that predicted by linear theory. It is observed that the lift force as well as in-line force increase with increasing frequency and waveheight.

In the above analysis the roughness parameter k' has been assumed to be very small since the cylinder material is aluminium. From the shore protection mannual (vol II), C_d, C_m and C_L are found to be 1.2, 2.0 and 3.3 respectively for all the six experiments for regular waves.

The recorded signals for the regular waves have been presented in the Figure 4.1. Visually it can be observed that force signals are not in phase with the water surface elevation signal.

A comparison of Table 4 and Table 5 shows that the lift force is more than the in-line force. This is due to the dynamic response of the cylinder which is not bottom-supported.

Random waves:

In Tables 6 and 7, rms values of forces and moments have been presented. It is observed that out of five peak frequencies chosen, the maximum rms value of in-line force and moment is attained at a peak frequency (fo) of 0.85 Hz. The lift force and moment decrease continuously with a drop in the magnitude of the peak frequency.

The spectral width parameter (ϵ) has been computed and tabulated in Tables 8 and 9. These are seen to be closer to unity and hence represent a near-Gaussian probability distribution function.

The recorded signals for random waves have been presented in Figure 4.2. Figure 4.3 shows the wave spectra for water surface elevation. Predicted and experimental spectra of the in-line forces and moments have been compared. This is shown in Figure 4.4 and Figure 4.5, respectively. The predicted spectra for forces and moments have been obtained from the formulas presented in section 2.2.4. Figures 4.6 and 4.7 show the spectra for forces and moments in the transverse (lift) direction, respectively. Lastly, Figure 4.8 represents the five harmonic components for drag and lift force and their phase difference with respect to water surface elevation.

A comparison between experimental in-line force spectrum and that predicted by linear theory can be seen in Figure 4.4. It can be inferred that at higher peak frequency, theoretical spectra

are close to the experimental spectra. In this present approach for the calculation of theoretical spectra, the values of drag constant (K_d) and inertia constant (K_i) have been assumed as constant at all depths of water in the flume. Despite this assumption there is a good agreement between theory and experiments.

Similar calculations have been carried out for the in-line moment in Figure 4.5. The same trend as in the case of in-line force is observed here. Spectral analysis shows that all the peaks of theoretical and experimental force and moment spectra are around the same respective frequencies.

Predictions for the lift force and moment spectra in case of random wave are not available. The experimentally obtained spectra for lift force and corresponding moment have been presented in Figures 4.6 and 4.7, respectively. As before, the peak of the force and moment spectra is around the same frequency as it is for corresponding water surface elevation spectra.

Figure 4.8 shows that the input water surface elevation signals and the corresponding force signals are not in phase and their harmonic components have phase differences.

Table 1

Parameters for Regular Wave Experiments

Experiment No.	Frequency Hz	Waveheight Cm
1	1.00	8.00
2	1.00	12.00
3	1.25	8.00
4	1.25	12.00
5	0.75	8.00
6	0.75	12.00

Table 2

Parameters for Random wave (Jonswap spectra) Experiments

$$S(f) = \frac{\alpha g^2}{(2\pi)^4 f^5} \exp\left[-\frac{5}{4}\left(\frac{f}{f_o}\right)^{-4}\right] \gamma^a$$

$$a = \exp\left[-(f-f_o)^2 / 2\sigma^2 f_o^2\right]$$

$$\sigma = \begin{cases} \sigma_a = 0.07 & \text{for } f \leq f_o \\ \sigma_b = 0.09 & \text{for } f > f_o \end{cases}$$

f_o = peak frequency (Hz)

α = 0.0081

g = 9.81 m/s^2

Experiment No.	Peak frequency f_o (Hz)	γ
7	0.75	5.00
8	0.85	5.00
9	1.00	5.00
10	1.10	5.00
11	1.25	5.00

Table 3

Raynolds numbers and Keulegan-Carpenter numbers

Expt. No.	f Hz	H cm	maximum surface velocity U_m cm/s	Reynolds No. $Re = \frac{U_m D}{\nu}$	Keulegan-Carpenter No. $K' = \frac{U_m T}{D}$
1	1.00	9.47	29.74	14872	5.95
2	1.00	12.60	39.60	19803	7.92
3	1.25	8.33	32.71	16356	5.23
4	1.25	10.89	42.76	21380	6.84
5	0.75	8.42	19.83	9919	5.29
6	0.75	13.23	31.17	15585	6.23

Table 4

Experimental and predicted in-line force and moment for regular wave experiments

Expt. No.	f (Hz)	Measured Wave height at SWL	Maximum In-line force		Maximum moment in In-line direction	
		cm	Experimental force (N)	Predicted force (N)	Experimental moment (Nm)	Predicted moment (Nm)
1	1.00	9.47	2.38	1.86	1.68	0.96%
2	1.00	12.60	3.85	2.56	2.88	1.39
3	1.25	8.33	3.55	1.61	2.99	0.94
4	1.25	10.89	4.85	2.17	4.23	1.30
5	0.75	8.42	2.08	1.57	1.39	0.70
6	0.75	13.23	4.21	2.54	3.35	1.20

Table 5

Experimental and predicted lift force and moment for regular waveexperiments

Expt. No.	f (Hz)	Wave height at SWL (cm)	Maximum Lift force		Maximum moment i Lift direction
			Experimental force (N)	Predicted force (N)	Experimental moment (Nm)
1	1.00	8.42	3.59	5.20	3.50
2	1.00	13.09	6.90	9.05	6.74
3	1.25	8.46	3.94	6.18	3.82
4	1.25	11.21	7.64	10.56	7.34
5	0.75	8.74	3.06	2.27	3.00
7	0.75	12.89	6.88	5.61	6.78

Table 6

Experimental rms value of In-line force and moment for random wave experiments

Expt. No.	Peak frequency f_o (Hz)	Rms value of water surface elevation measured at SWL (cm)	Rms value of In-line force (N)	Rms value of In-line moment (Nm)
7	0.75	2.34	0.42	0.56
8	0.85	1.84	0.98	0.83
9	1.00	1.33	0.50	0.32
10	1.10	1.11	0.41	0.26
11	1.25	0.84	0.31	0.20

Table 7

Experimental rms value of Lift force and moment for random waves experiments

Expt. No.	Peak frequency f_o (Hz)	Rms value of water surface Elevation measured at SWL (cm)	Rms value of lift force (N)	Rms value of lift moment (Nm)
7	0.75	2.31	1.55	1.51
8	0.85	1.81	1.26	1.23
9	1.00	1.32	0.86	0.84
10	1.10	1.11	0.61	0.59
11	1.25	0.83	0.51	0.49

Table 8

Spectral width parameters for In-line force and moment

Expt. No.	Water surface Elevation	Force	Moment
	ϵ	ϵ	ϵ
7	0.77	0.79	0.78
8	0.72	0.65	0.65
9	0.65	0.85	0.86
10	0.60	0.84	0.84
11	0.57	0.87	0.87

Table 9

Spectral width parameters for Lift force and moment

Expt. No.	Water surface Elevation	Lift Force	Moment in transverse direction
	ϵ	ϵ	ϵ
7	0.73	0.92	0.92
8	0.70	0.90	0.90
9	0.62	0.90	0.90
10	0.60	0.92	0.92
11	0.56	0.89	0.89

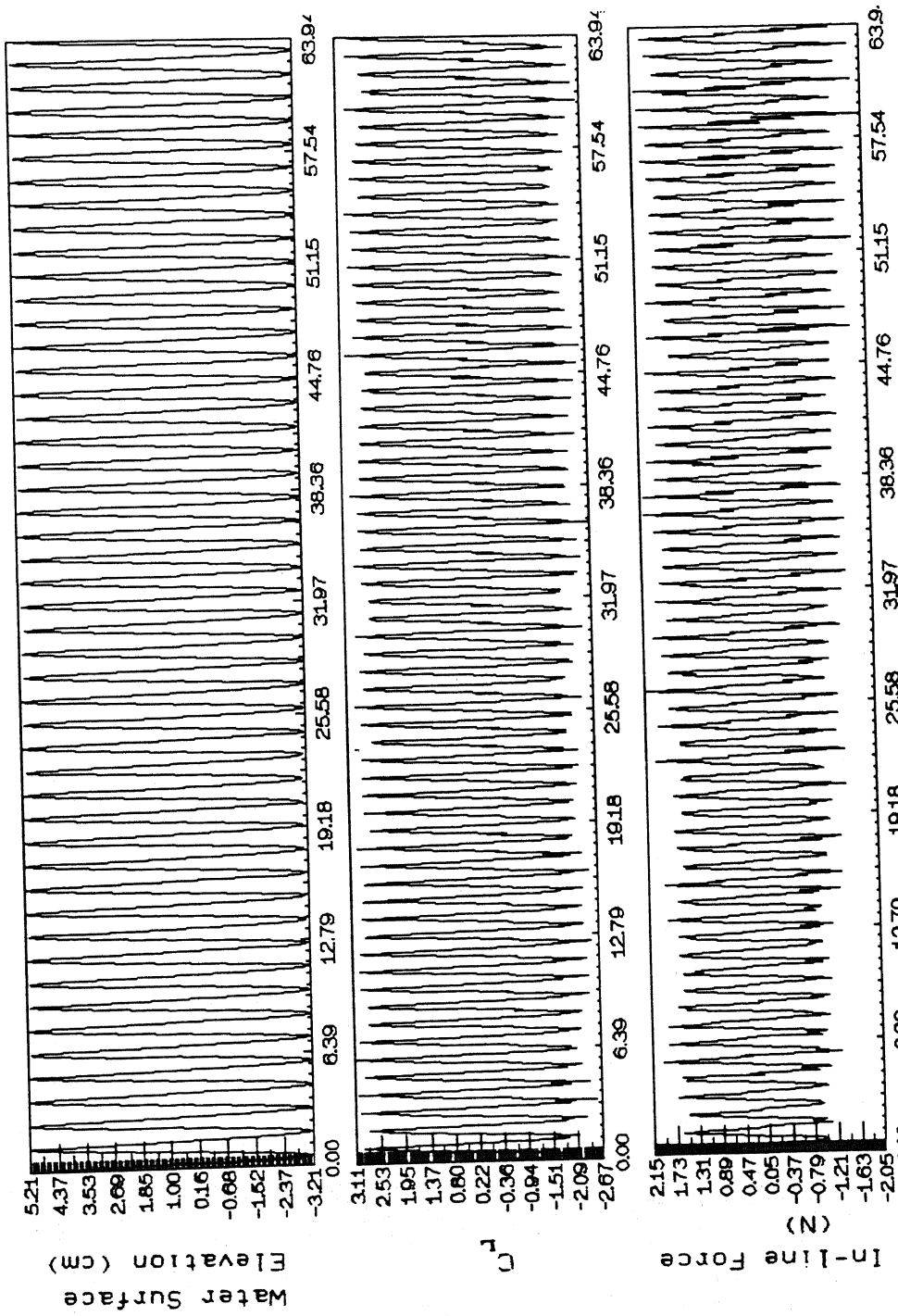

Fig. 4.1.a Measured Signals of Water Surface Elevation, Lift Coefficient and In-line Force for Expt. 1 (Regular Waves)

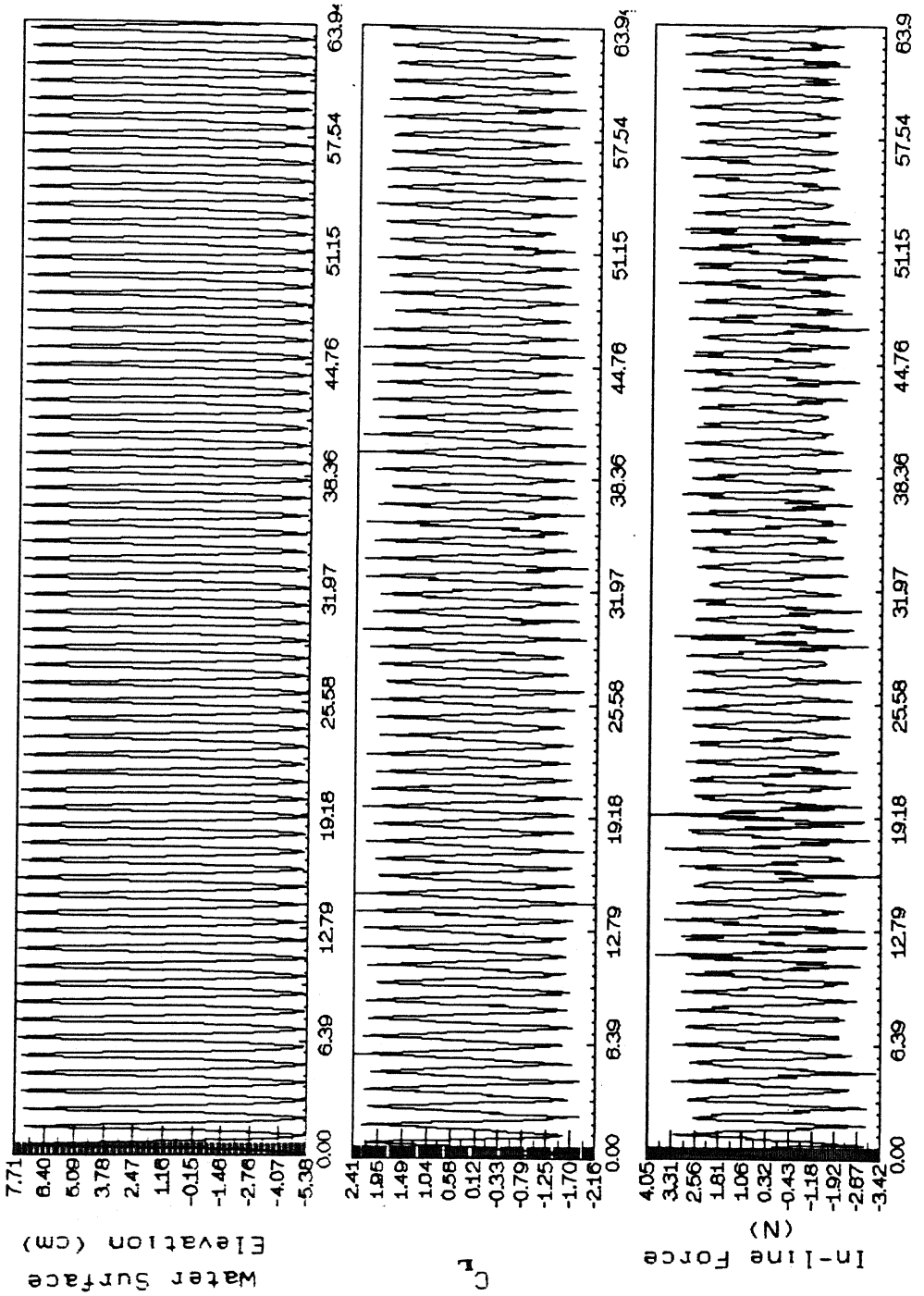

Fig. 4.1.b Measured Signals of Water Surface Elevation, Lift Coefficient and In-line Force for Expt. 2 (Regular Waves)

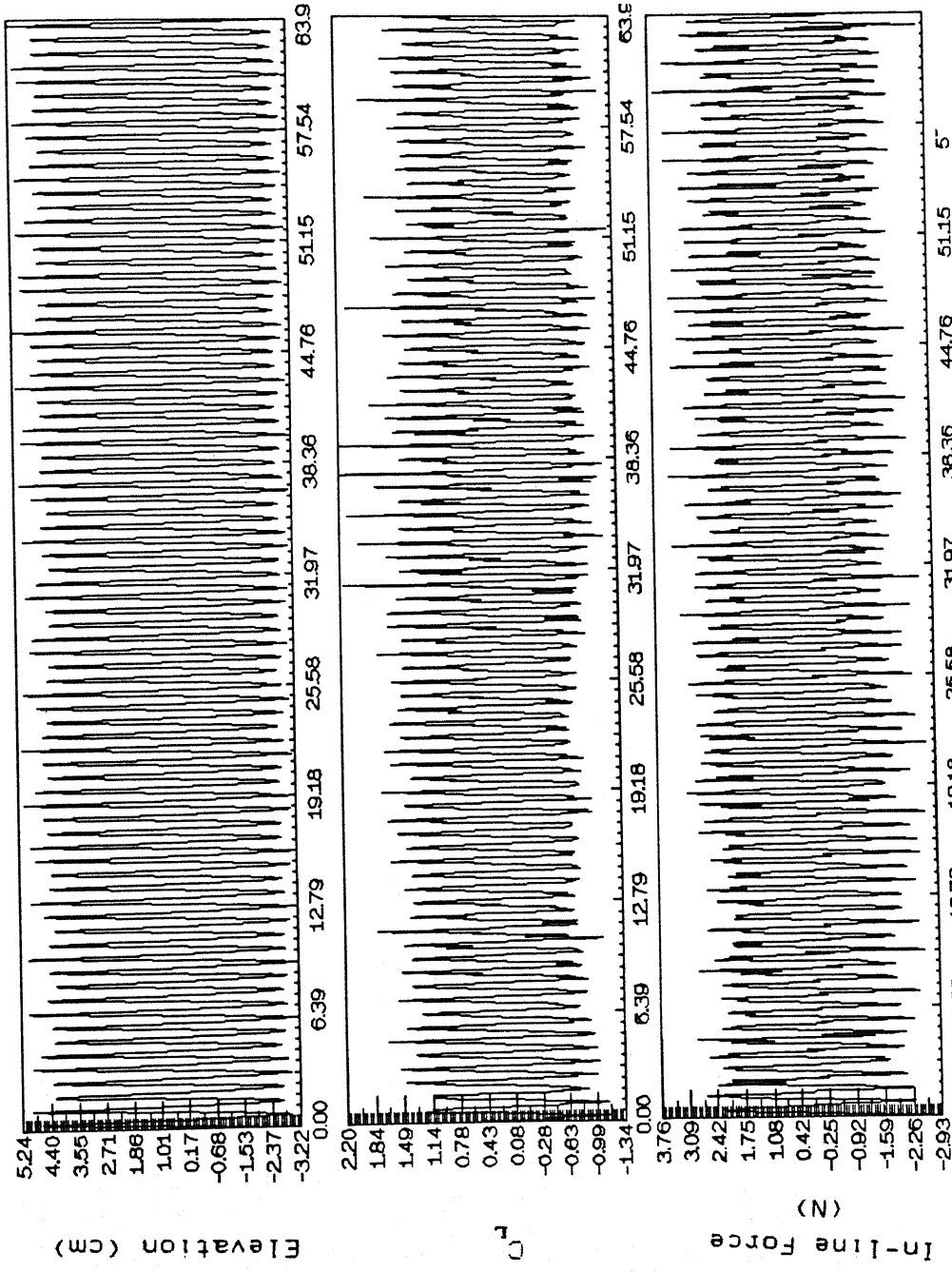

Fig. 4.1.c Measured Signals of Water Surface Elevation, Lift Coefficient and In-line Force for Expt. 3 (Regular Waves)

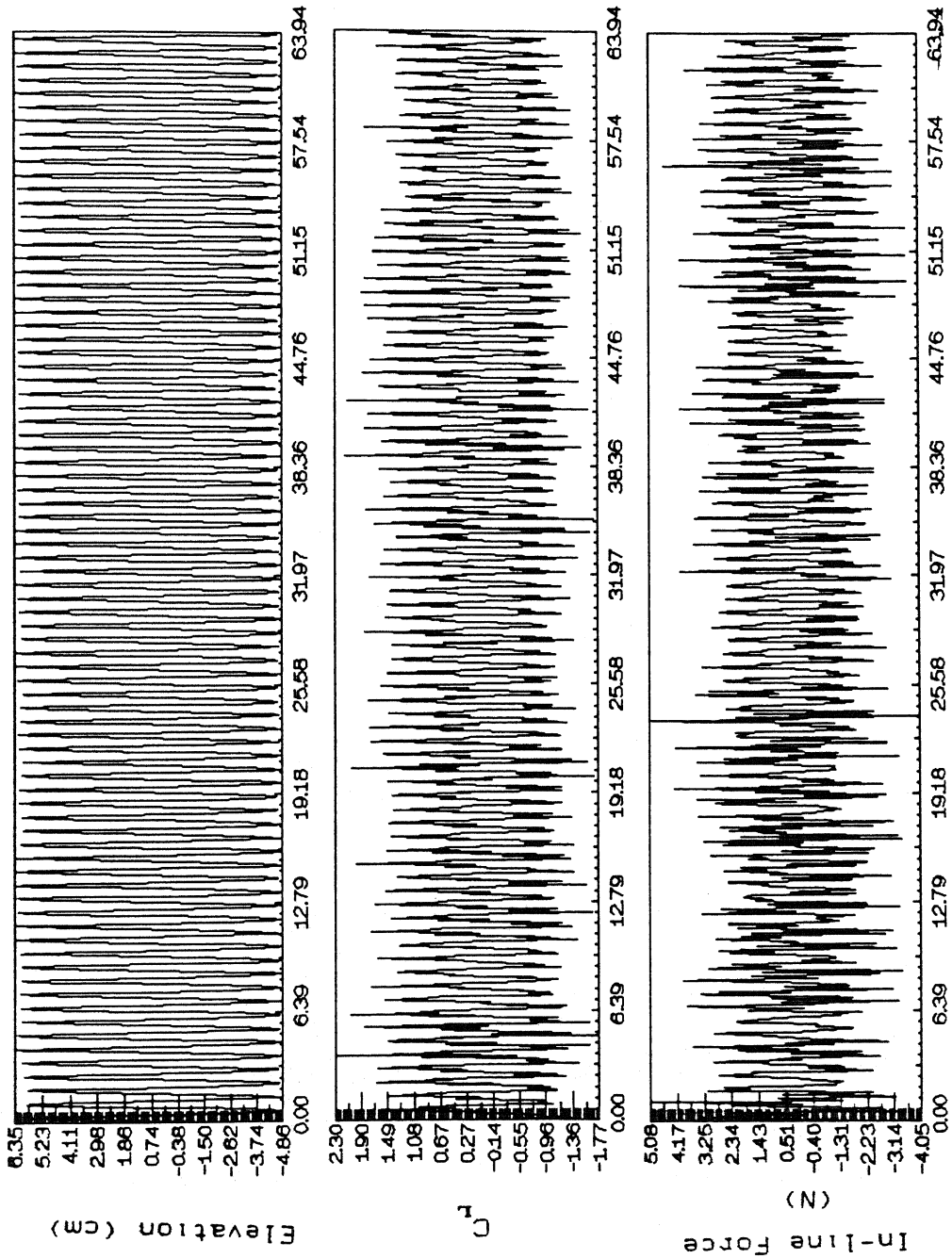

Fig. 4.1.d Measured Signals of Water Surface Elevation, Lift Coefficient and In-line Force for Expt. 4 (Regular Waves)

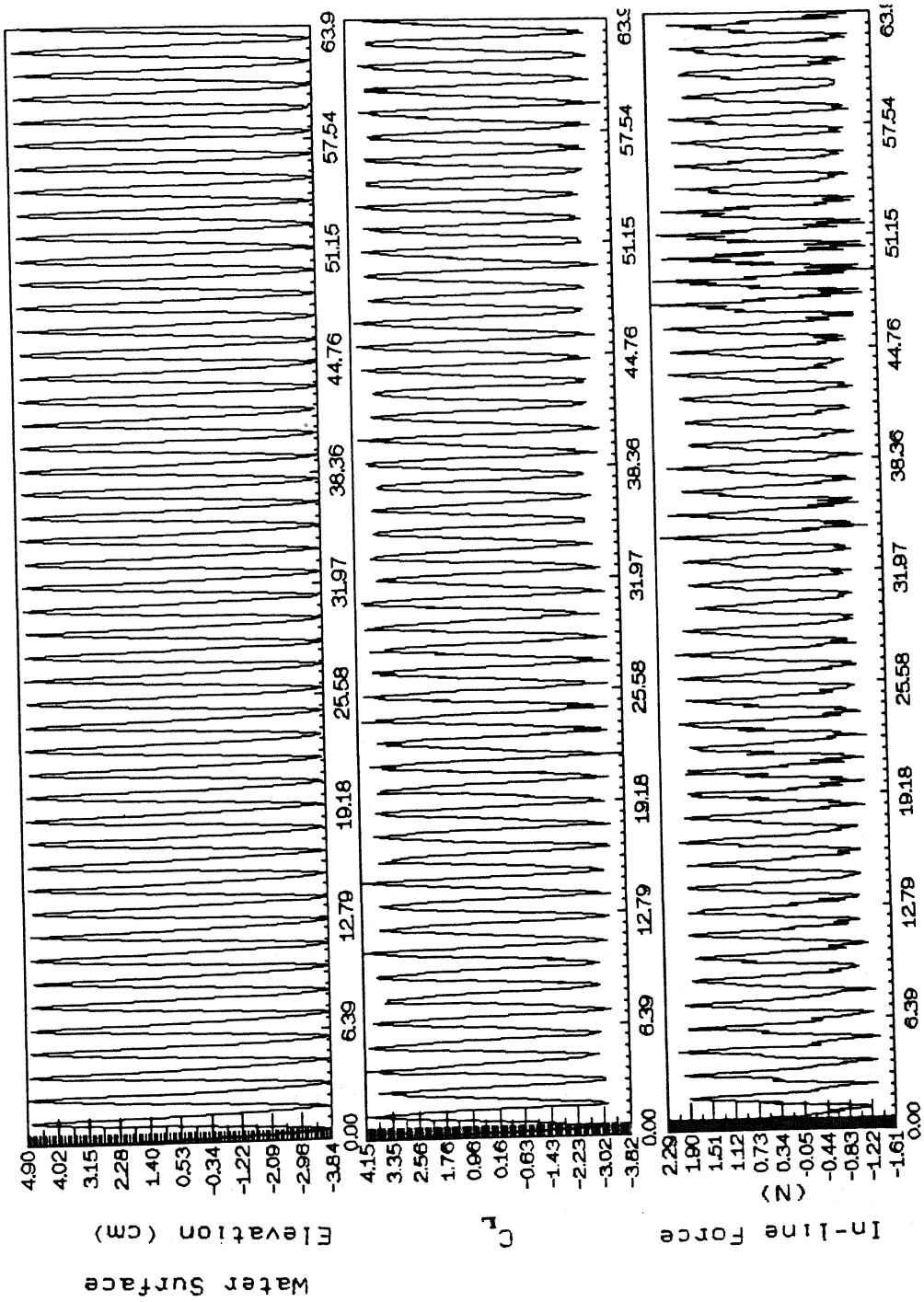

Fig. 4.1.e Measured Signals of Water Surface Elevation, Lift Coefficient and In-line Force for Expt. 5 (Regular Waves)

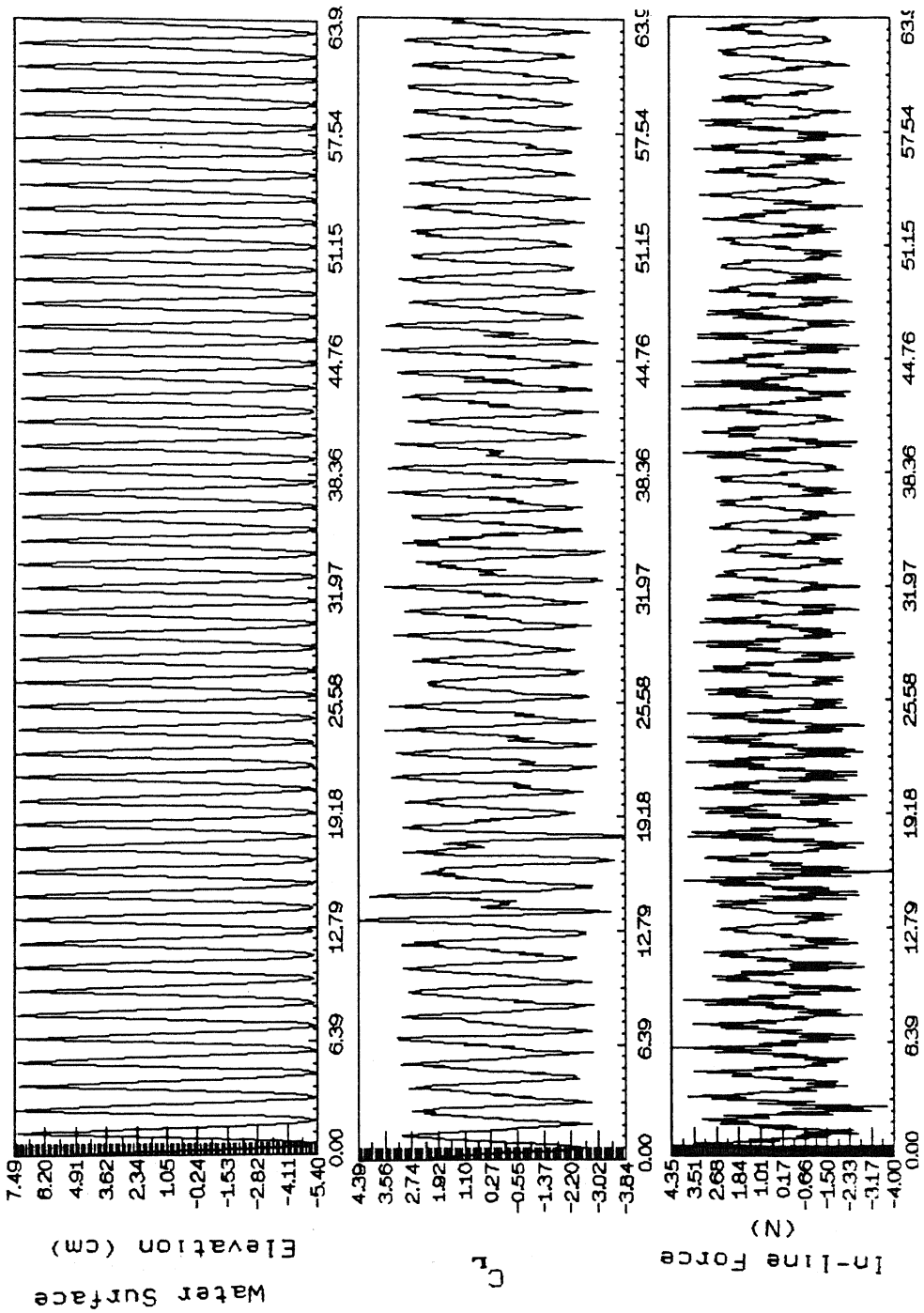

Fig. 4.1.f Measured Signals of Water Surface Elevation, Lift Coefficient and In-line Force for Expt. 6 (Regular Waves)

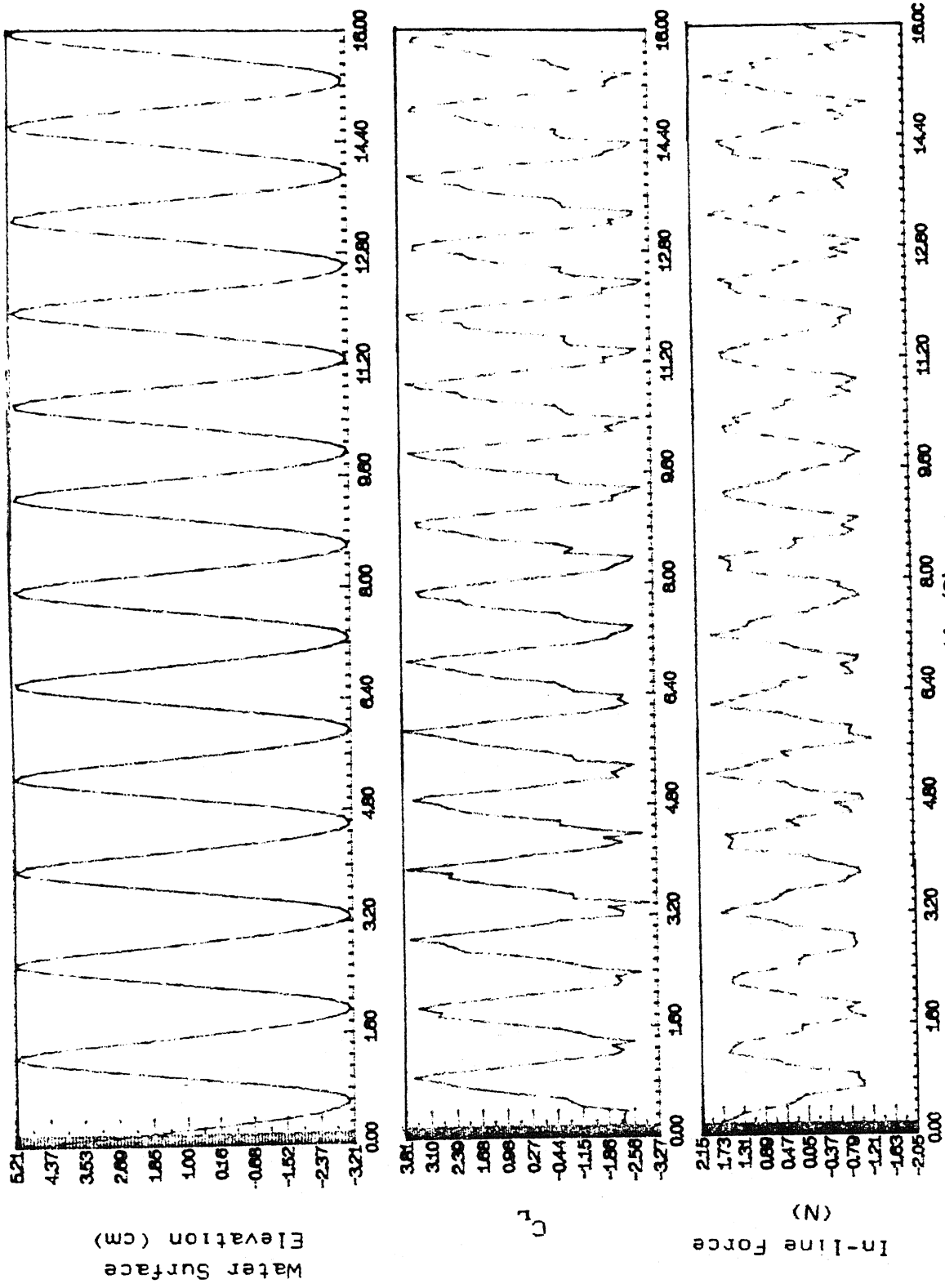

Fig. 4.1.g Expanded Form of Fig. 4.1.a

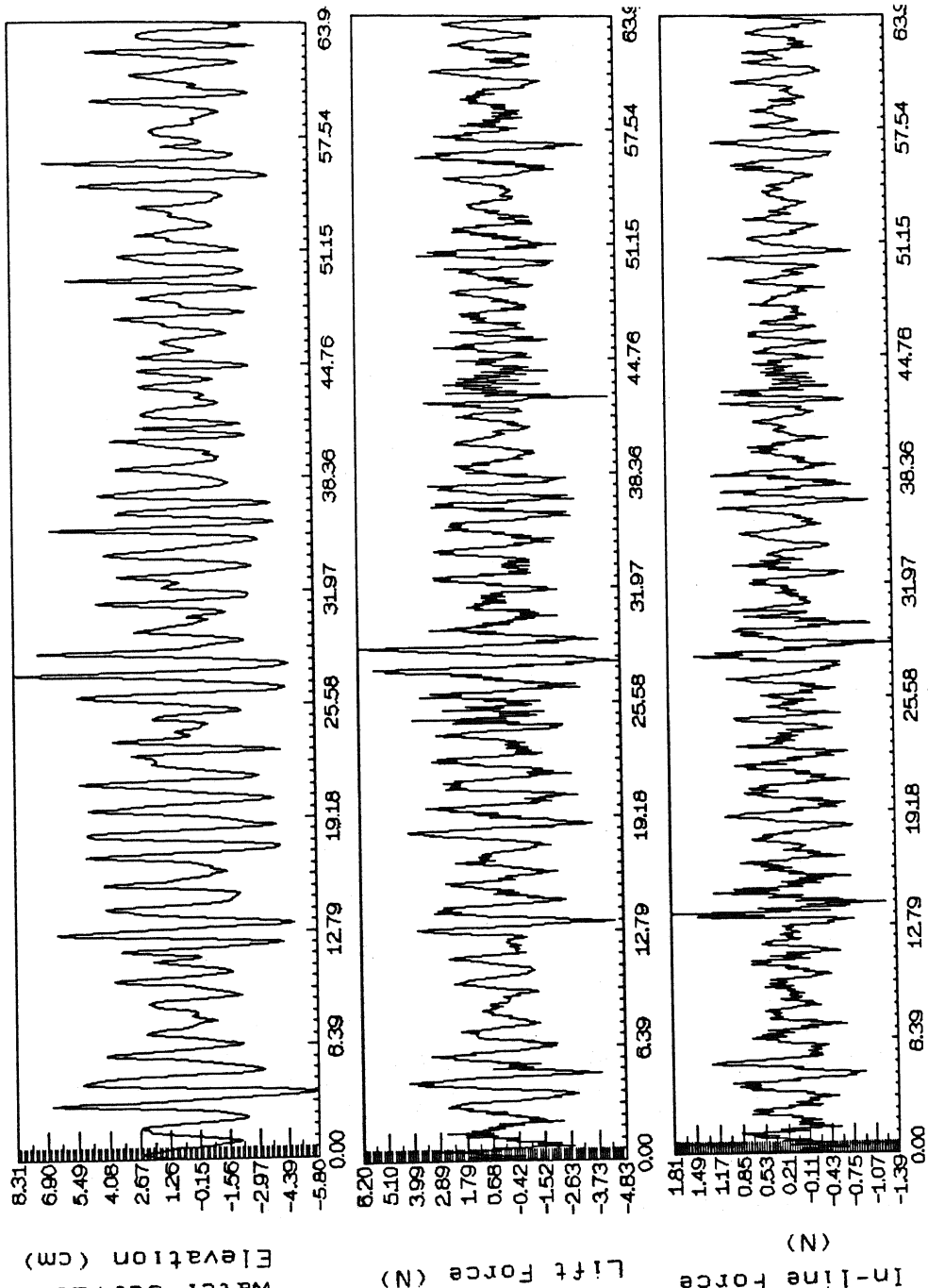

Fig. 4.2.a Measured Random Wave Signals of Water Surface Elevation, Lift Force and In-line Force for Expt. 7 (f_0 = 0.75 Hz)

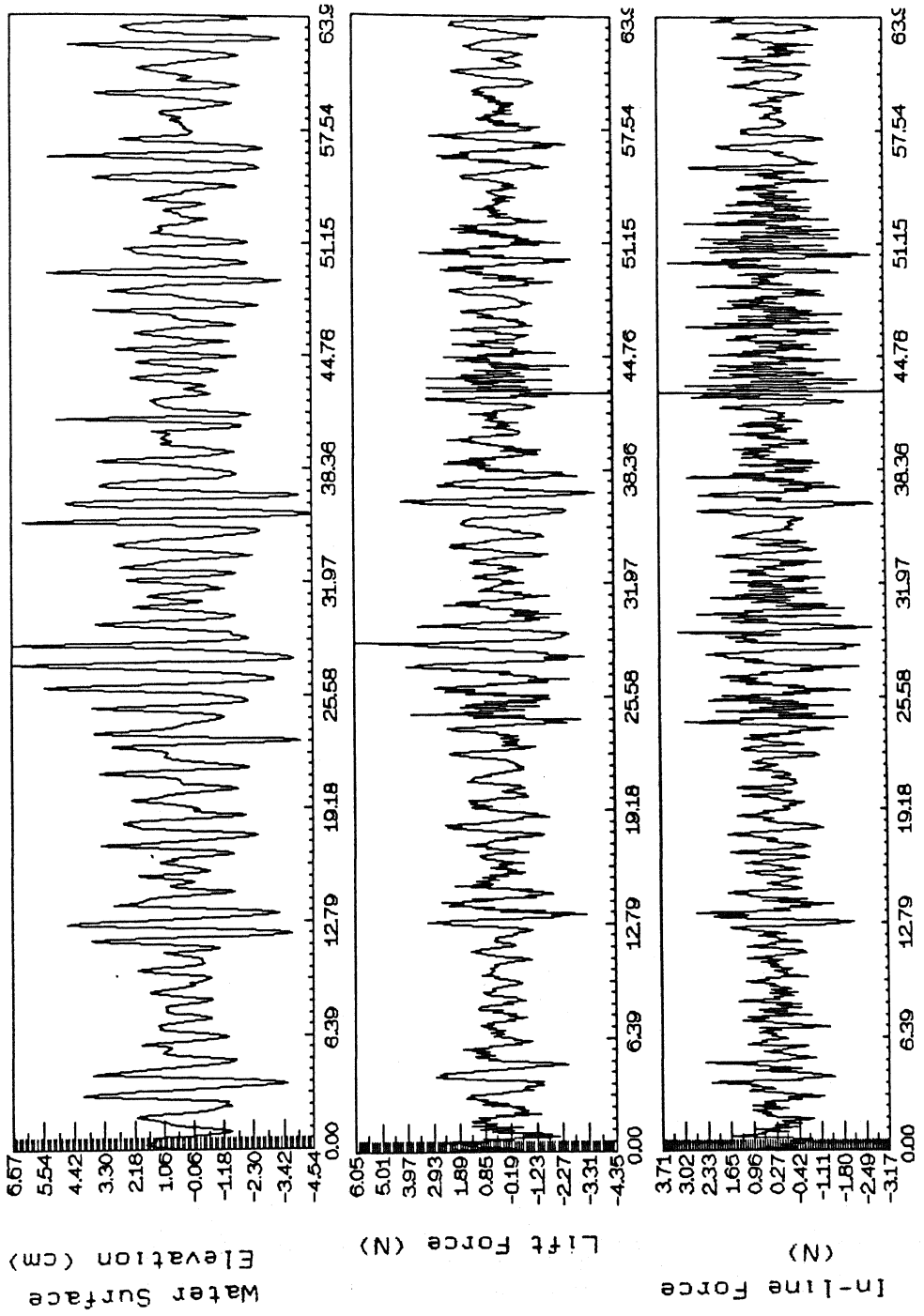

Fig. 4.2.b Measured Random Wave Signals of Water Surface Elevation, Lift Force and In-line Force for Expt. 8 (f_0 = 0.85 Hz)

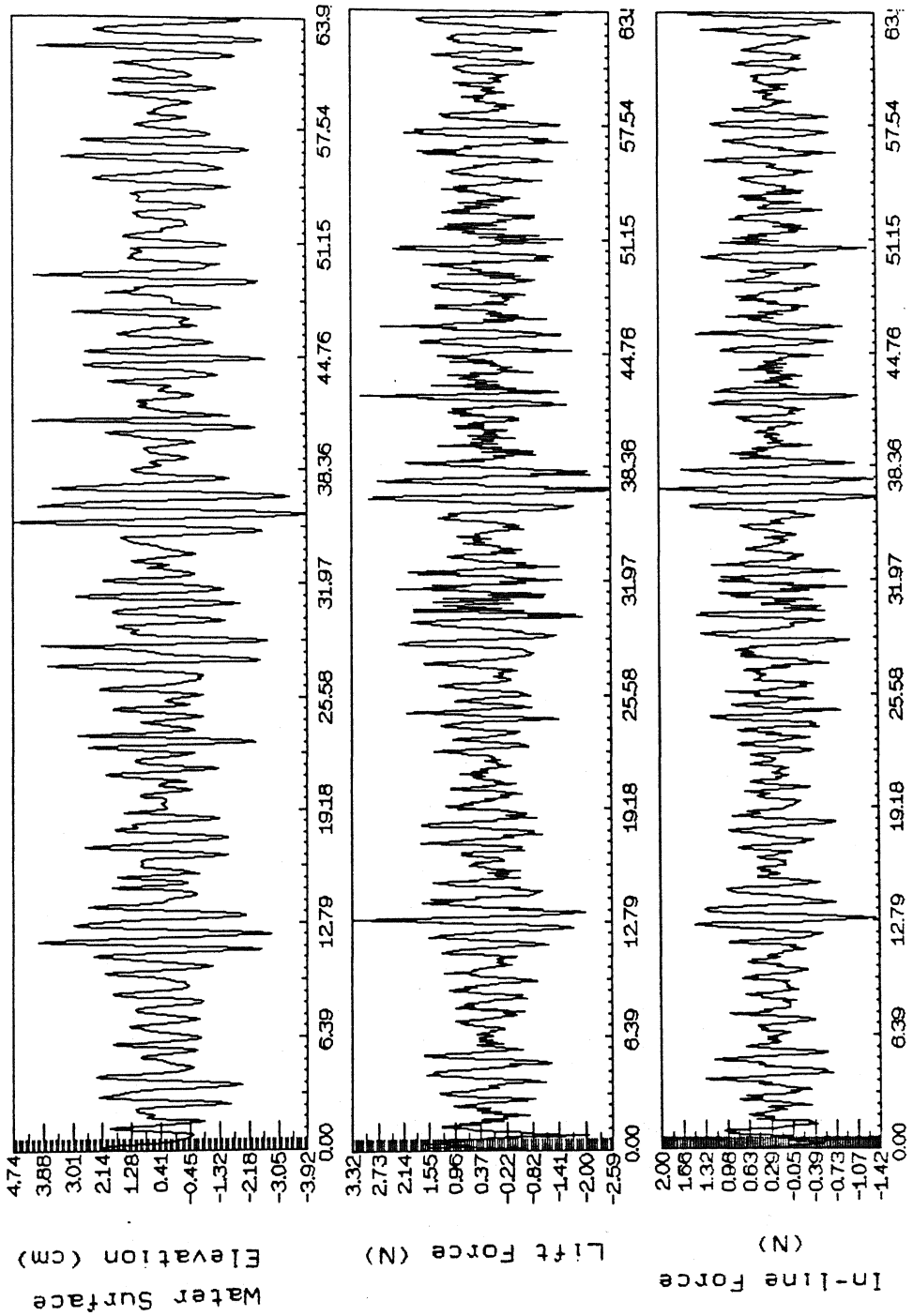

Fig. 4.2.c Measured Random Wave Signals of Water Surface Elevation, Lift Force and In-line Force for Expt. 9 (f_n = 1.00 Hz)

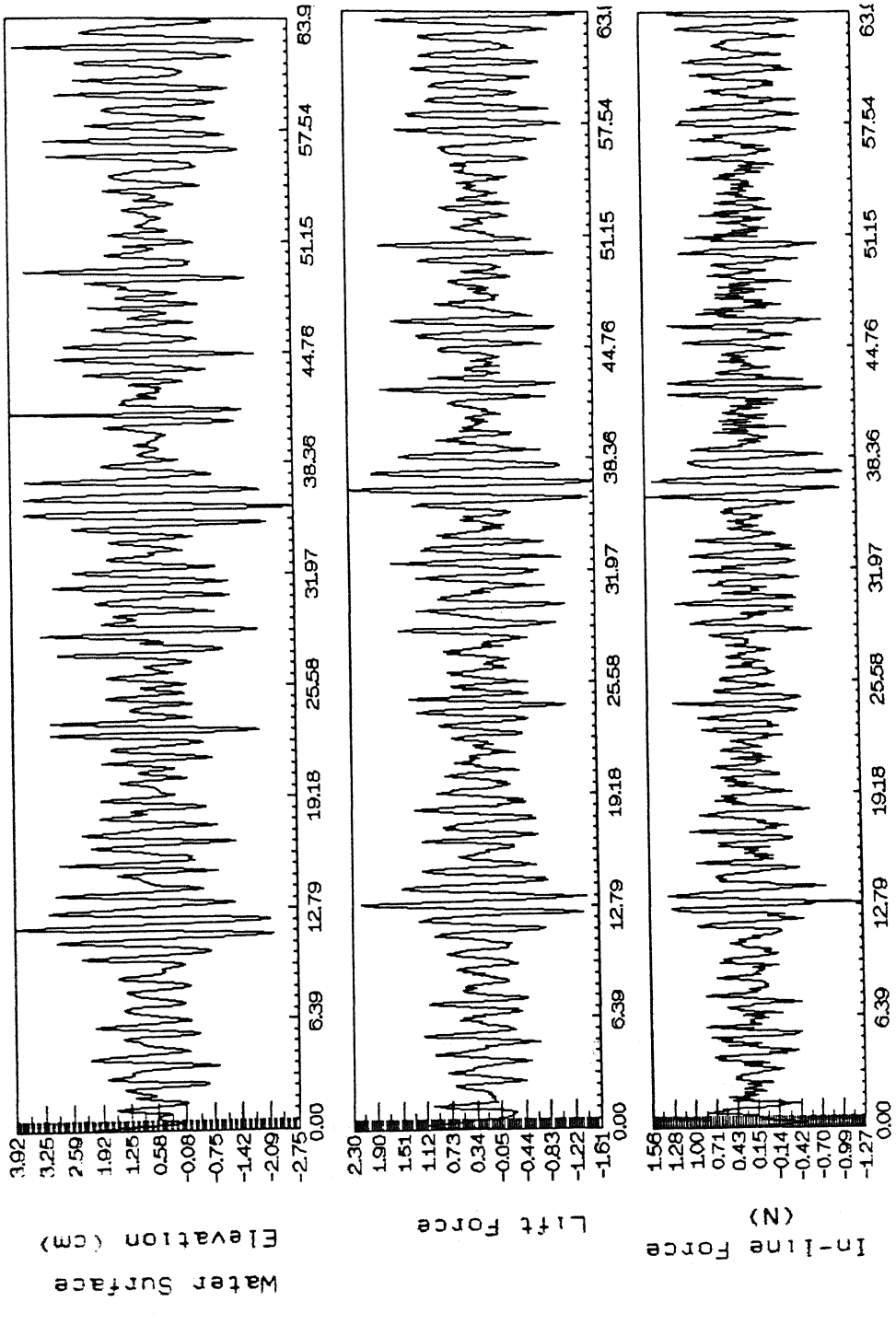

Fig. 4.2.d Measured Random Wave Signals of Water Surface Elevation, Lift Force and In-line Force for Expt. 10 (f_0 = 1.10 Hz)

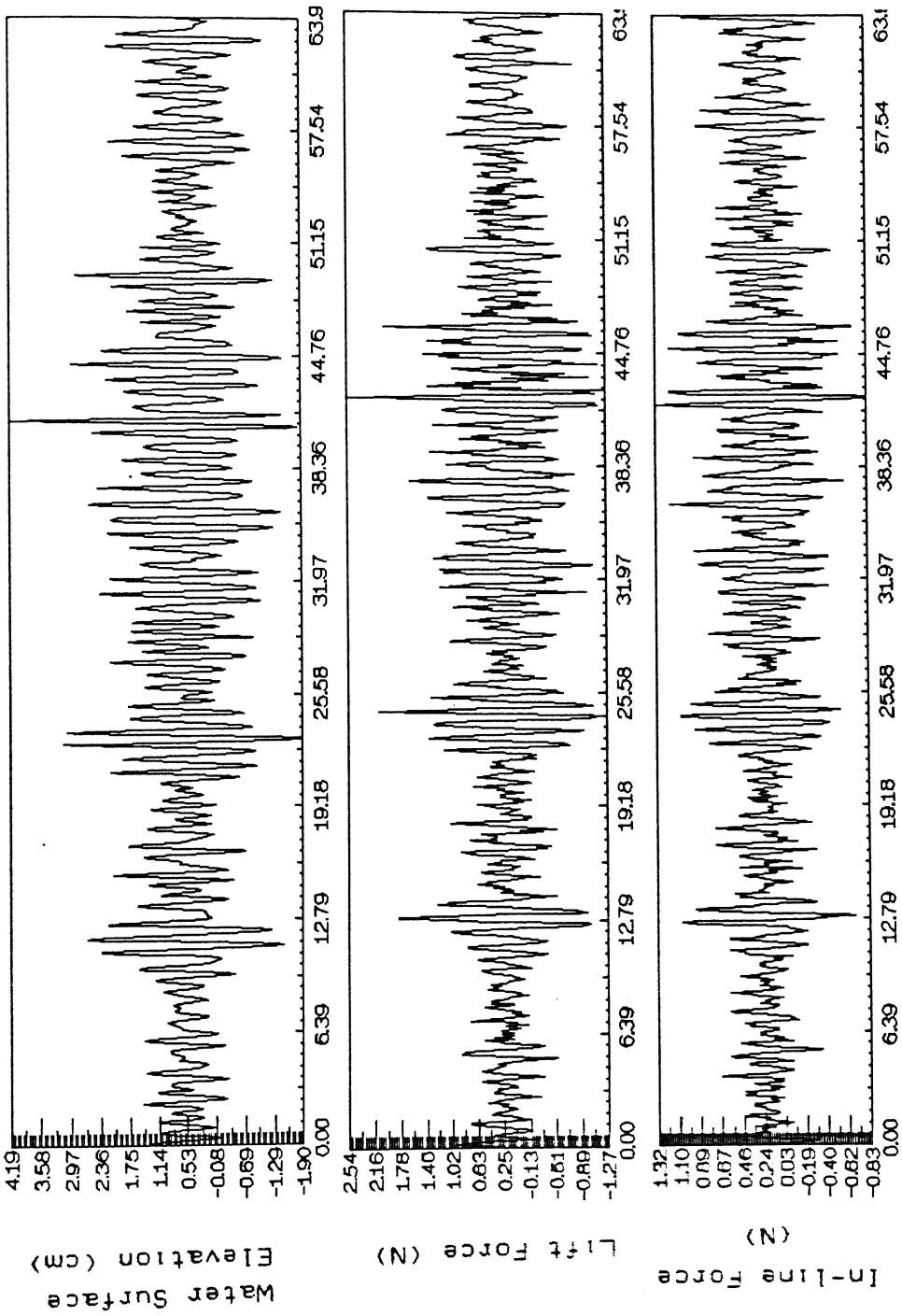

Fig. 4.2.e Measured Random Wave Signals of Water Surface Elevation, Lift Force and In-line Force for Expt. 11 (f_0 = 1.25 Hz)

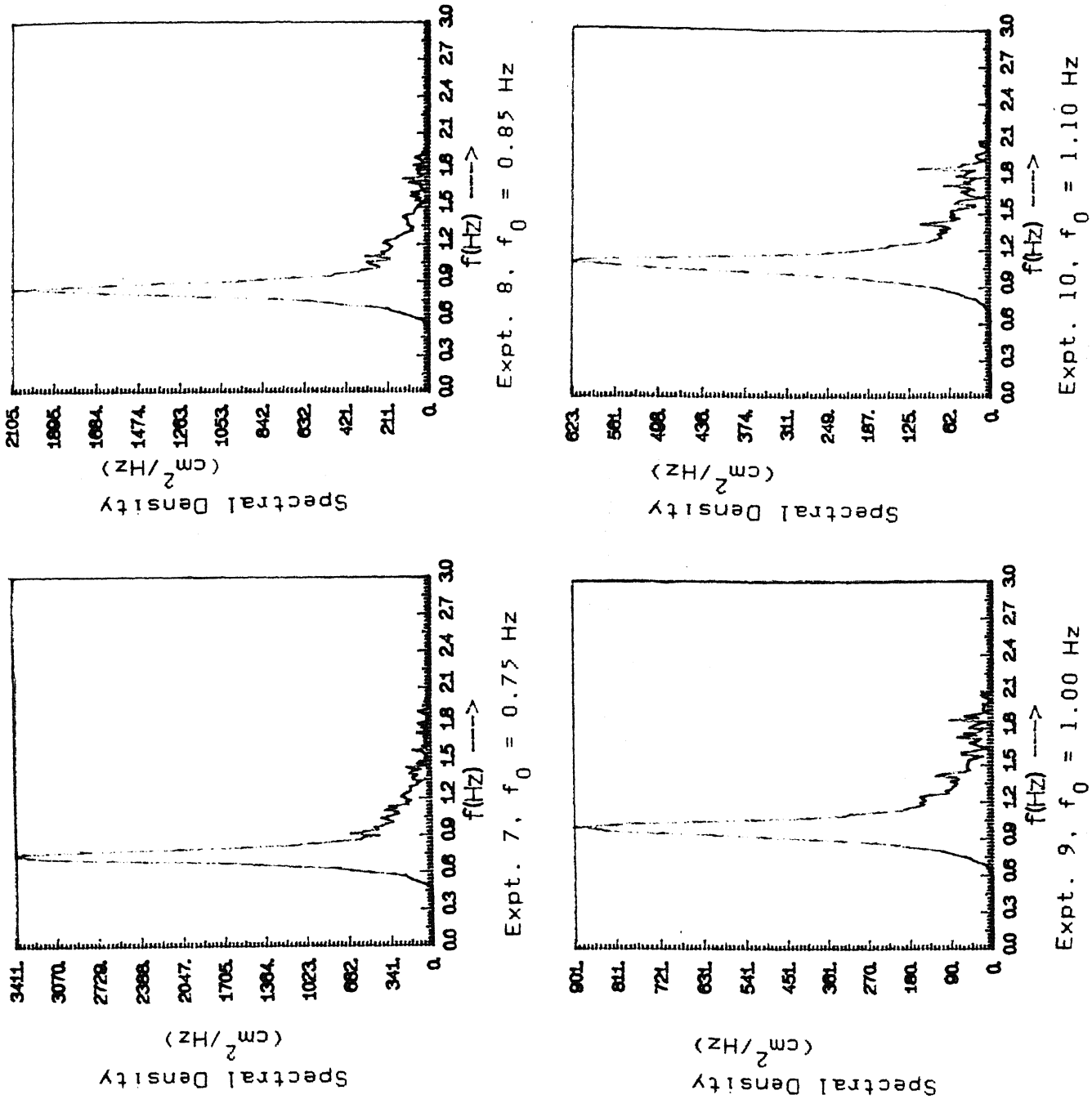

Fig. 4.3.a Wave Spectra for Expt. 7 to Expt. 10

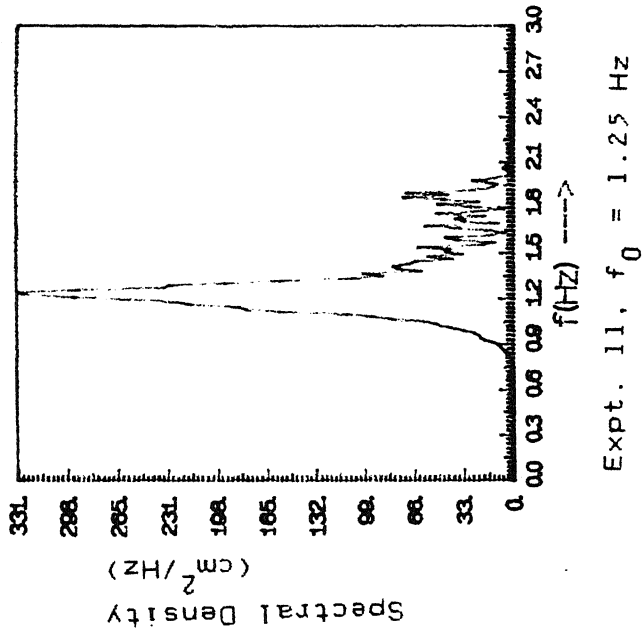

Fig. 4.3.b Wave Spectra for Expt. 11

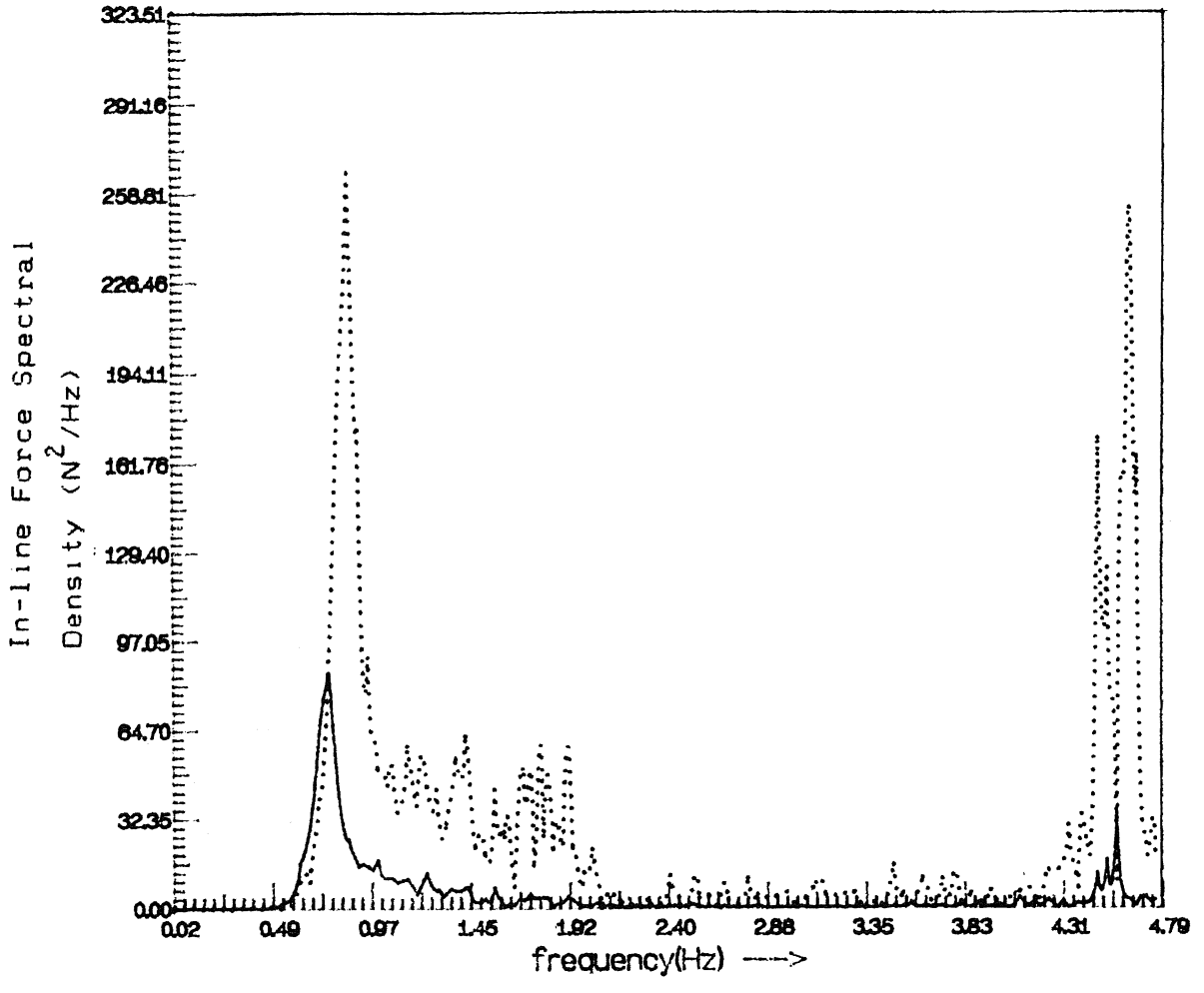

Fig. 4.4.a A Comparison between Experimental and Predicted In-line Force Spectra for Expt. 7 (f_0 = 0.75 Hz)
(Dotted line represents the predicted curve)

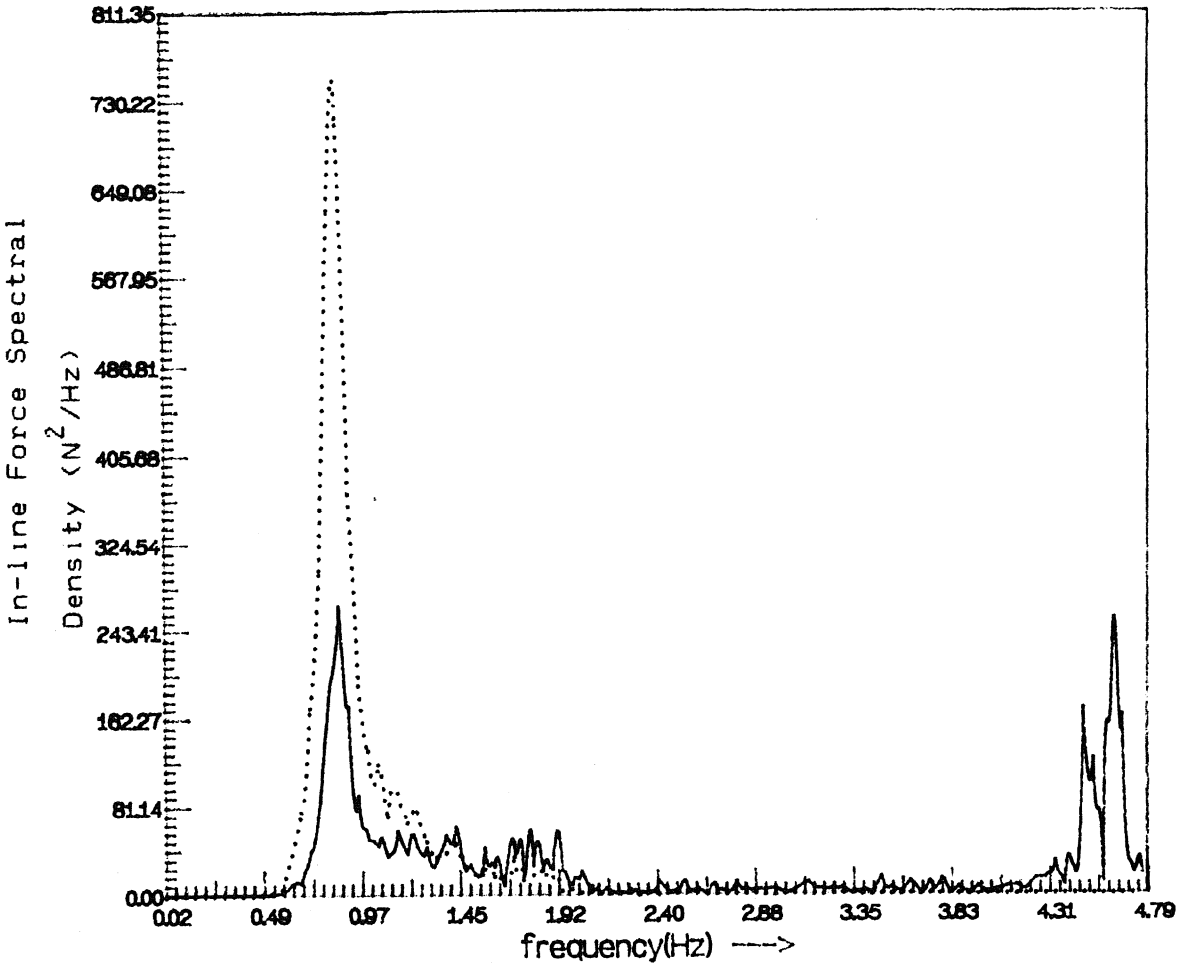

Fig. 4.4.b A Comparison between Experimental and Predicted In-line Force Spectra for Expt. 8 (f_0 = 0.85 Hz)
(Dotted line represents the predicted curve)

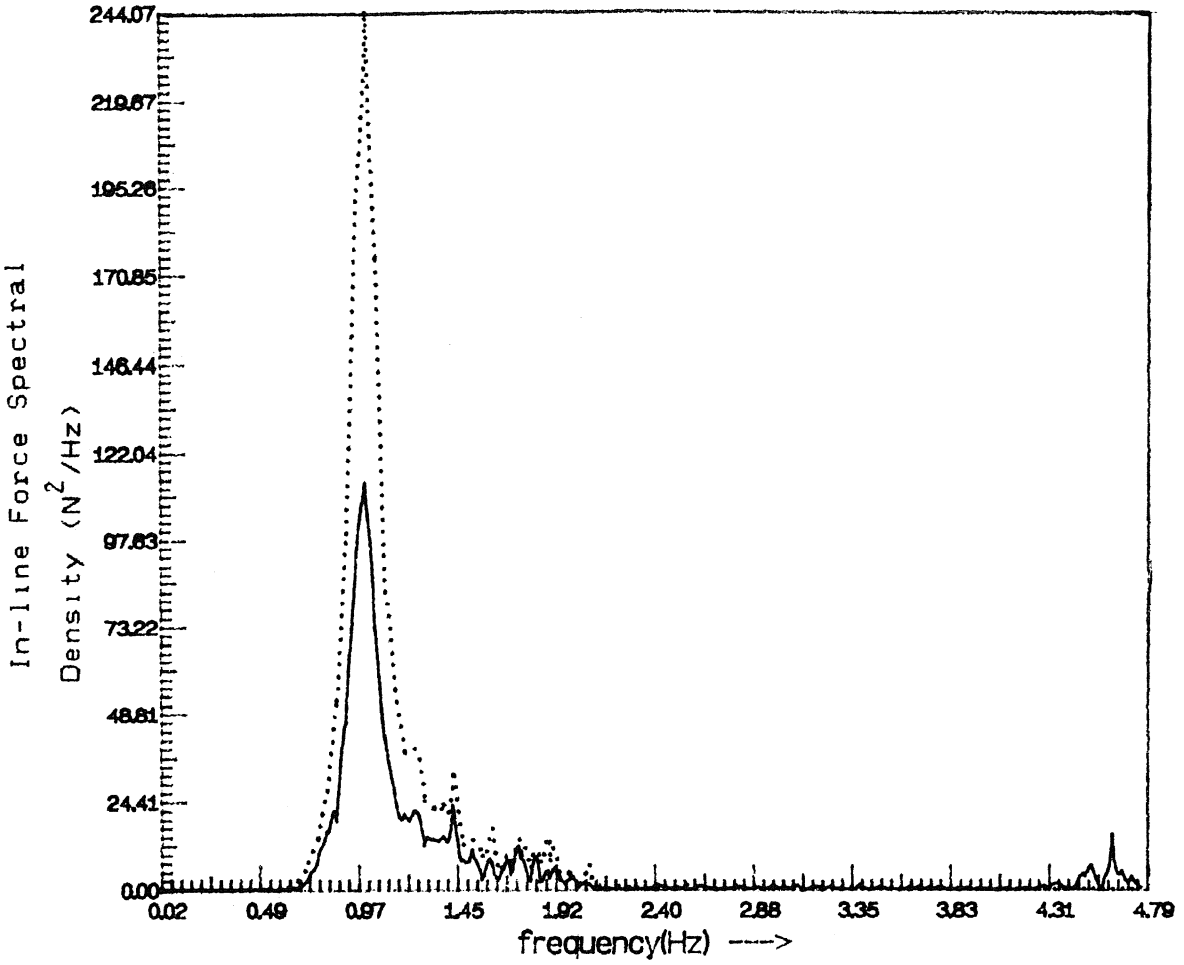

Fig. 4.4.c A Comparison between Experimental and Predicted In-line Force Spectra for Expt. 9 (f_0 = 1.00 Hz)
(Dotted line represents the predicted curve)

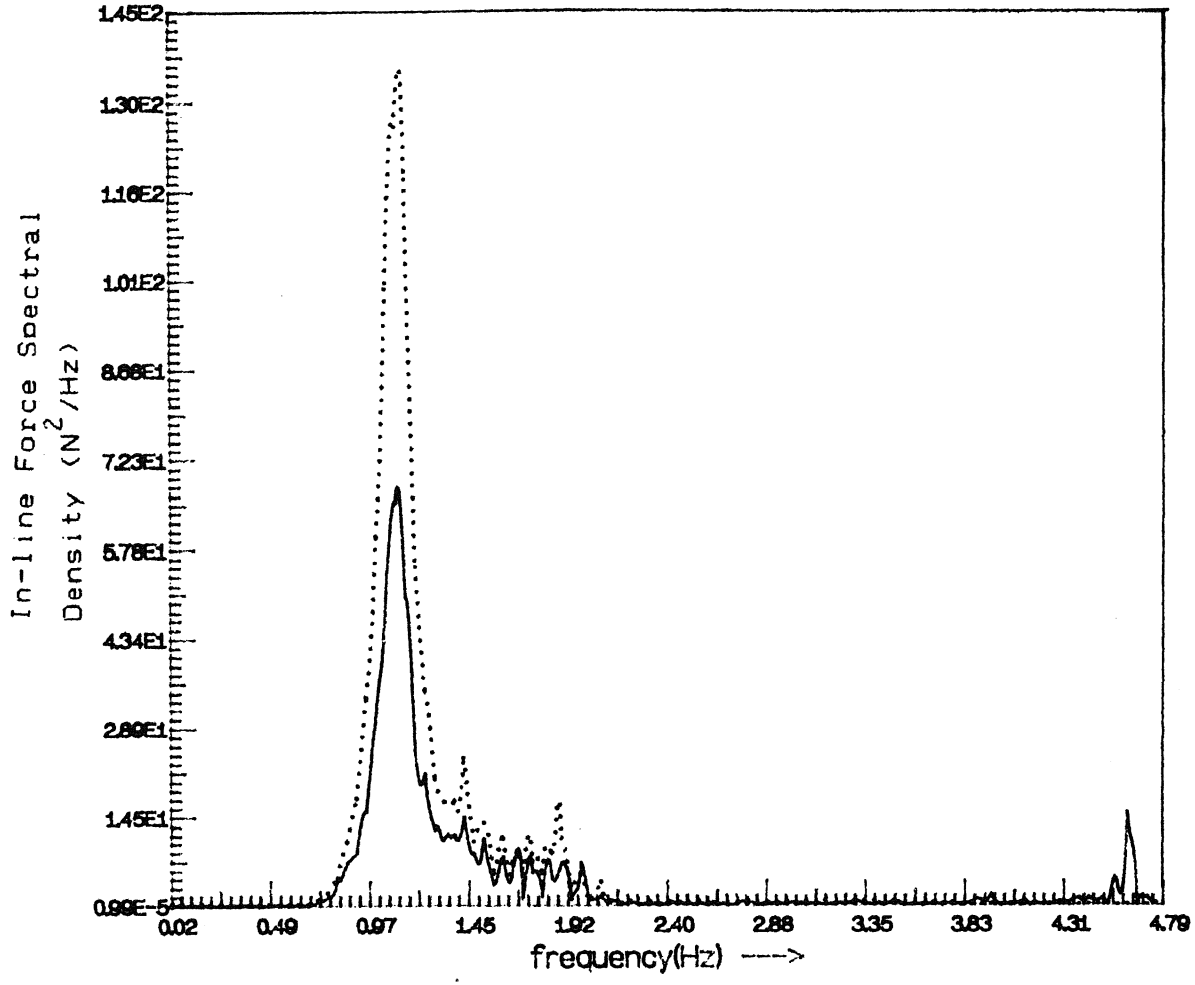

Fig. 4.4.d A Comparison between Experimental and Predicted In-line Force Spectra for Expt. 10 (f_0 = 1.10 Hz)
(Dotted line represents the predicted curve)

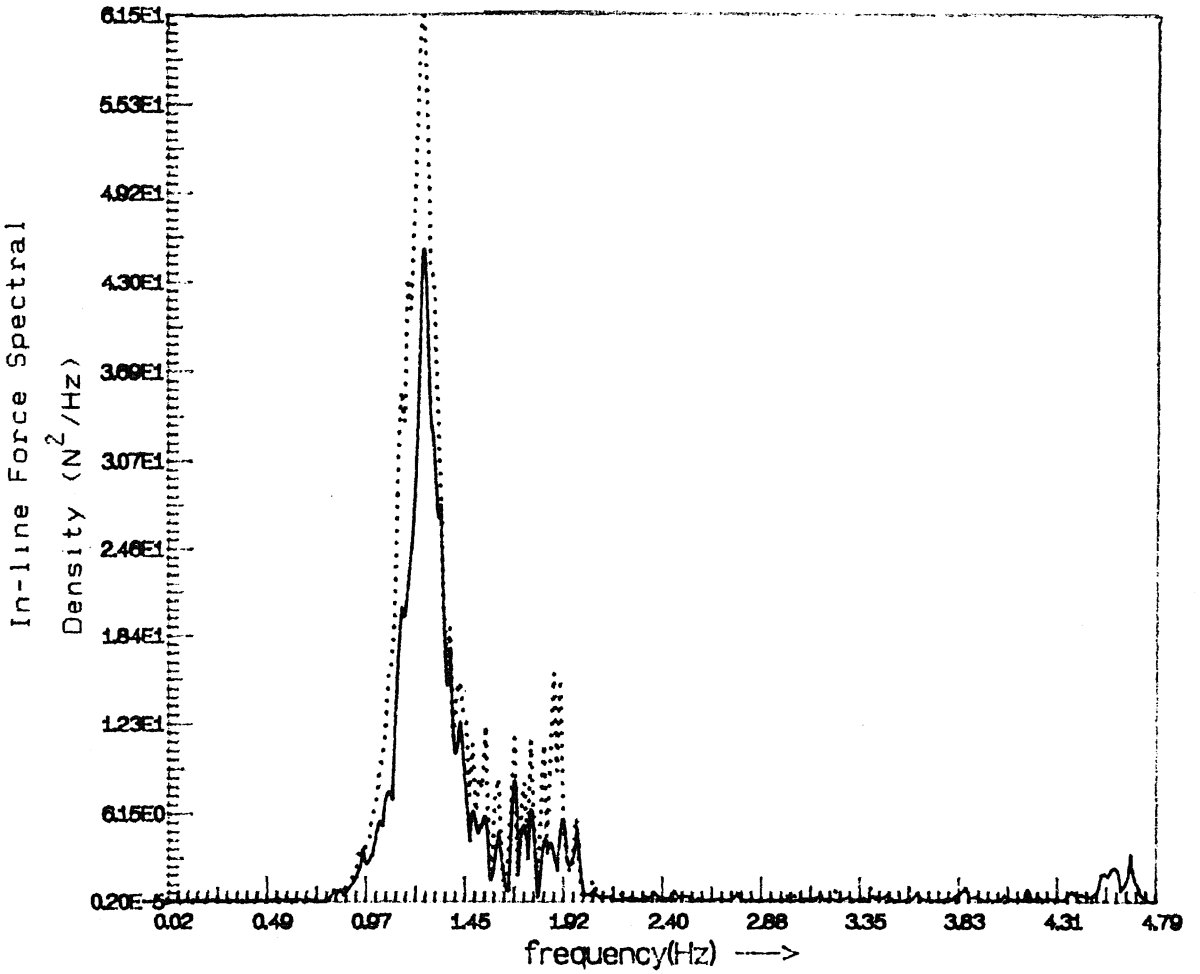

Fig. 4.4.e A Comparison between Experimental and Predicted In-line Force Spectra for Expt. 11 (f_0 = 1.25 Hz)
(Dotted line represents the predicted curve)

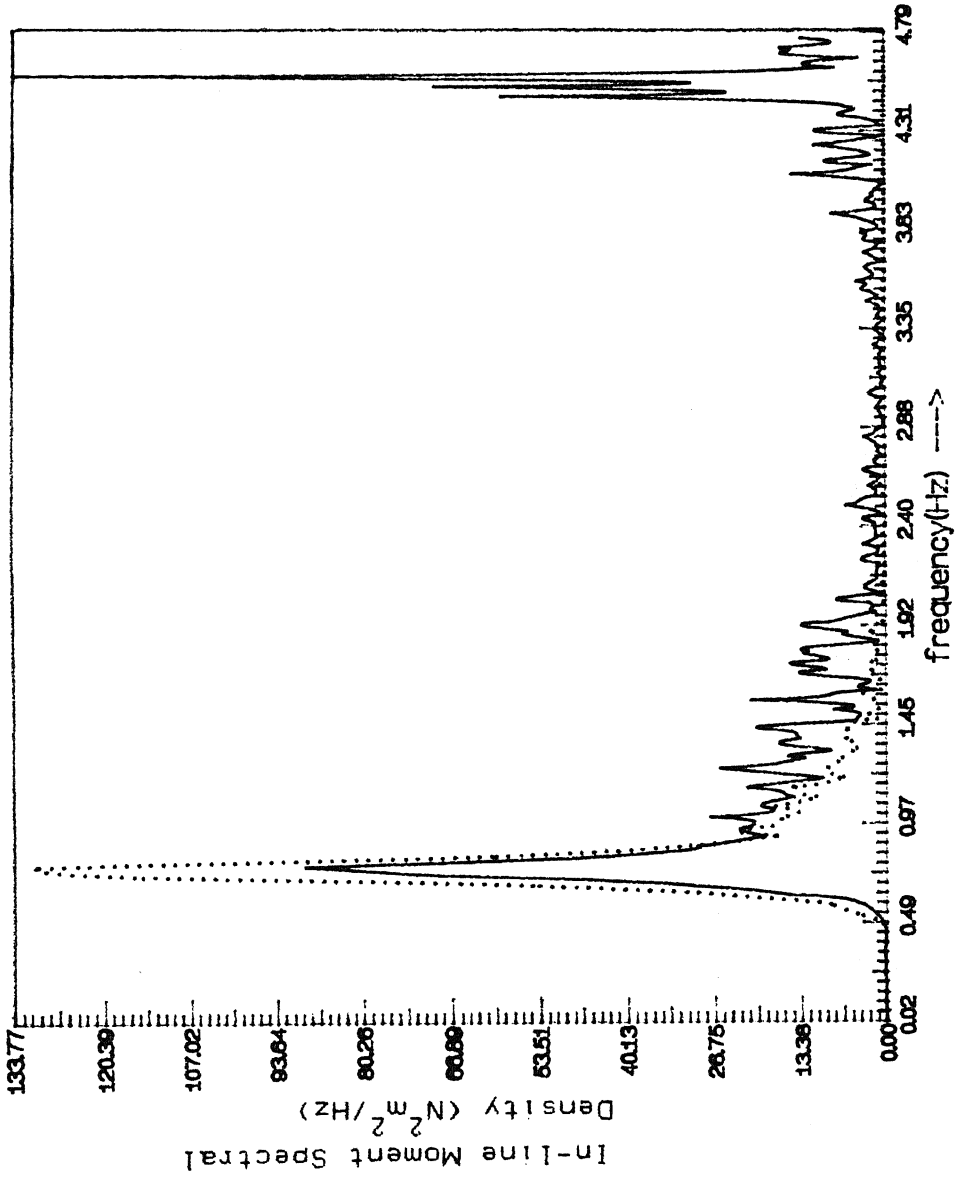

Fig. 4.5.a A Comparison between Experimental and Predicted In-line Moment Spectra for Expt. 7 (f_0 = 0.75 Hz)
(Dotted line represents the predicted curve)

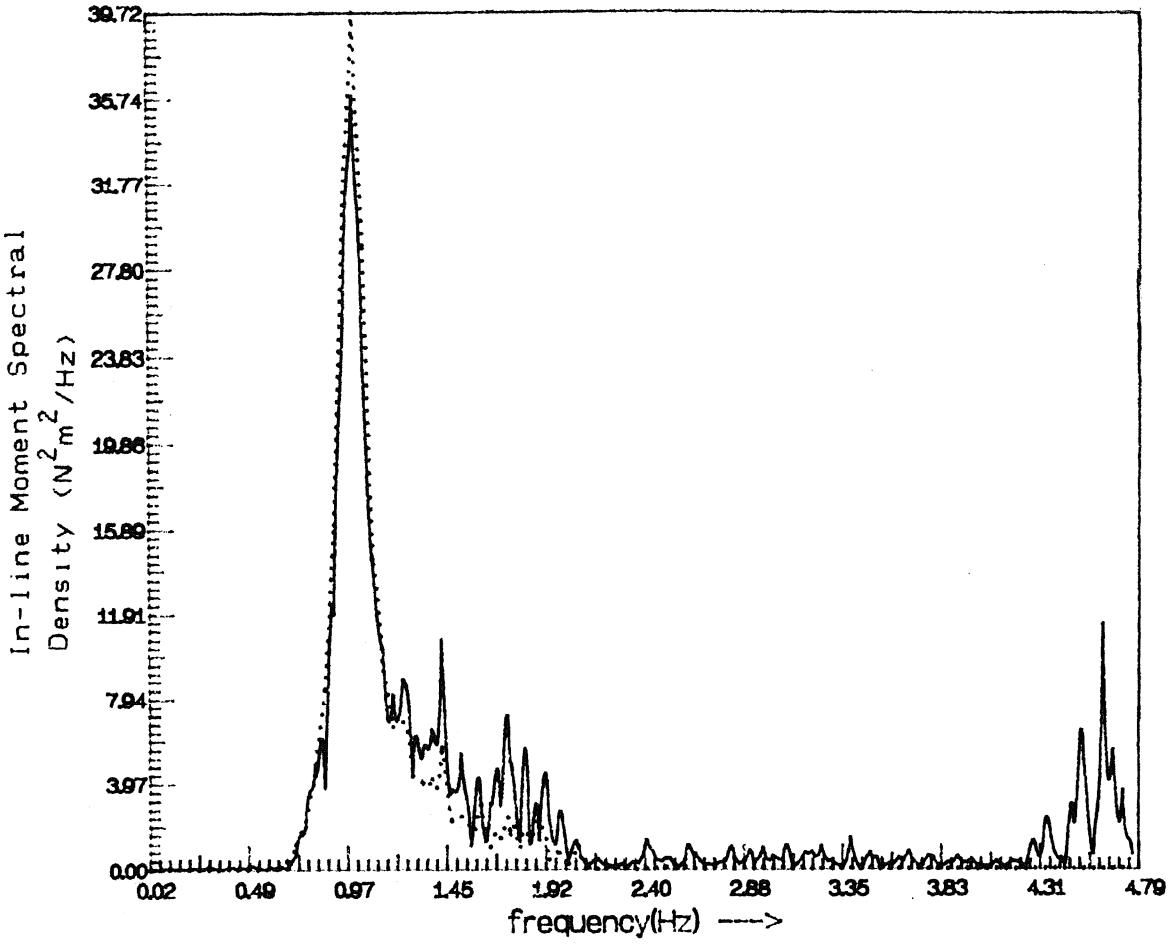

Fig. 4.5.c A Comparison between Experimental and Predicted In-line Moment Spectra for Expt. 9 (f_0 = 1.00 Hz)

(Dotted line represents the predicted curve)

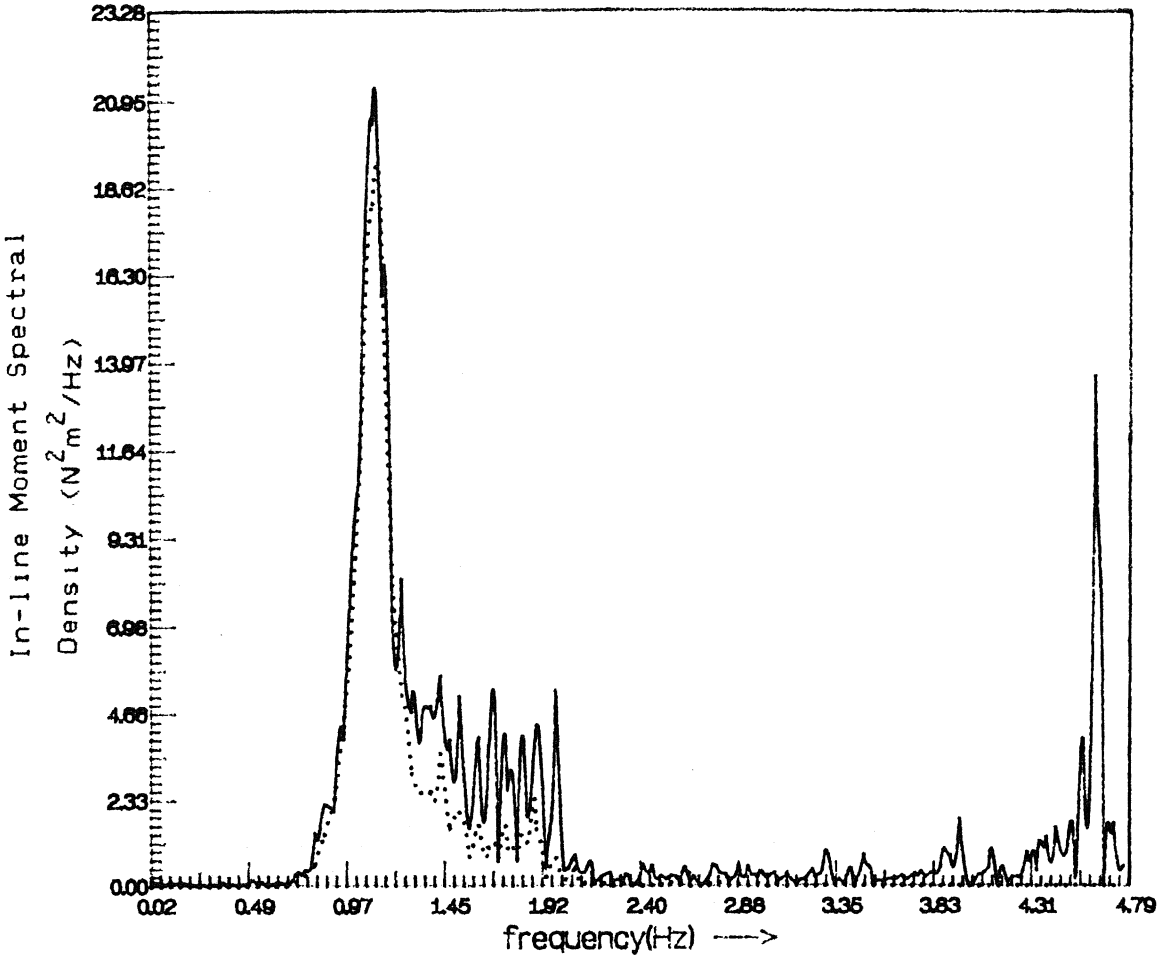

Fig. 4.5.d A Comparison between Experimental and Predicted In-line Moment Spectra for Expt. 10 (f_0 = 1.10 Hz)
(Dotted line represents the predicted curve)

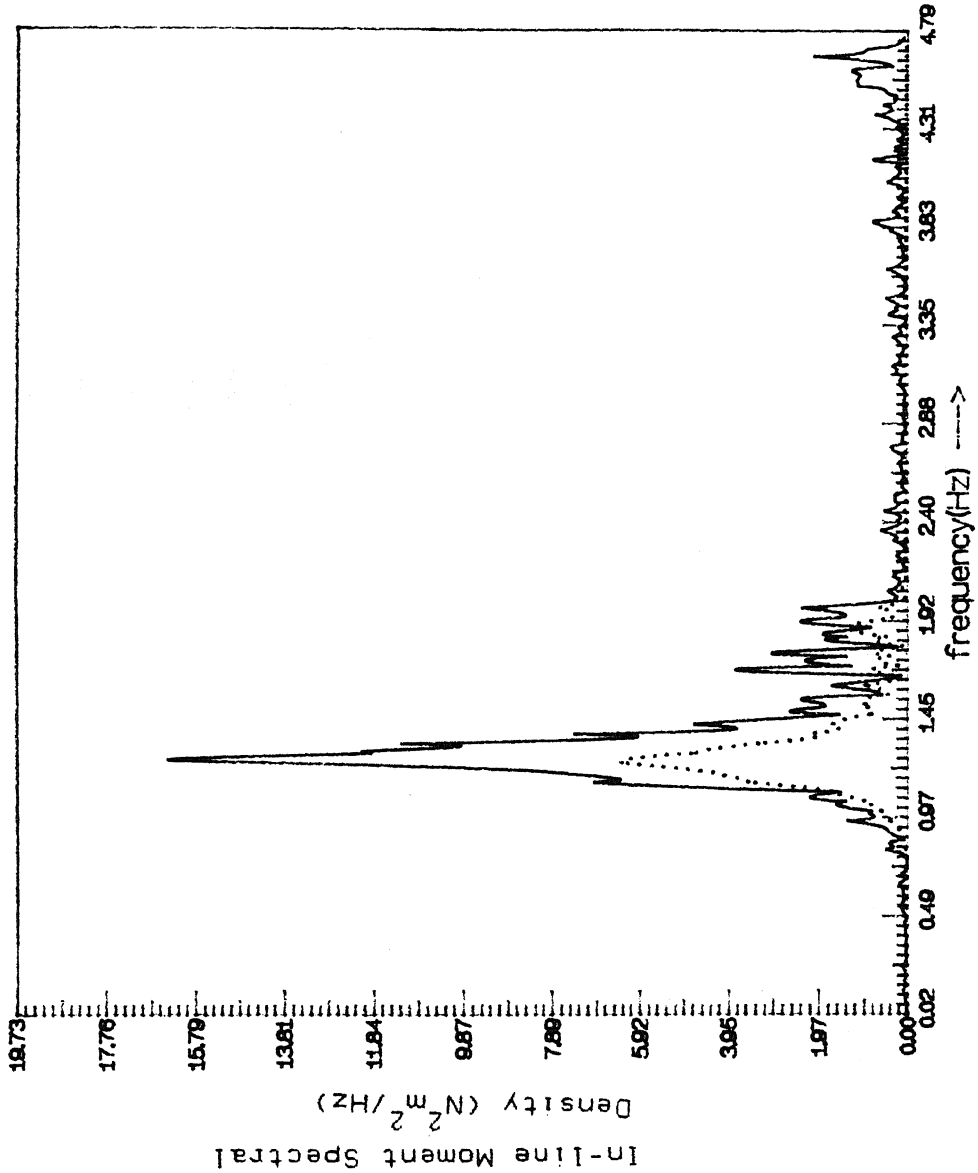

Fig. 4.5.e A Comparison between Experimental and Predicted In-line Moment Spectra for Expt. 11 (f_0 = 1.25 Hz)
(Dotted line represents the predicted curve)

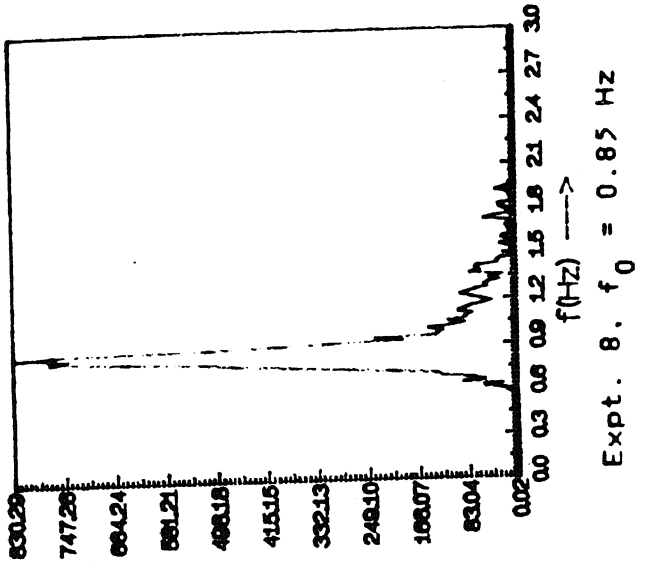

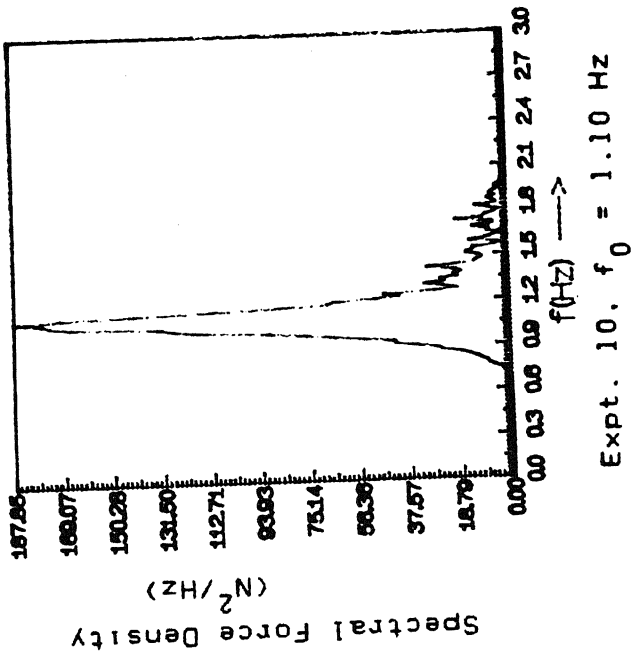

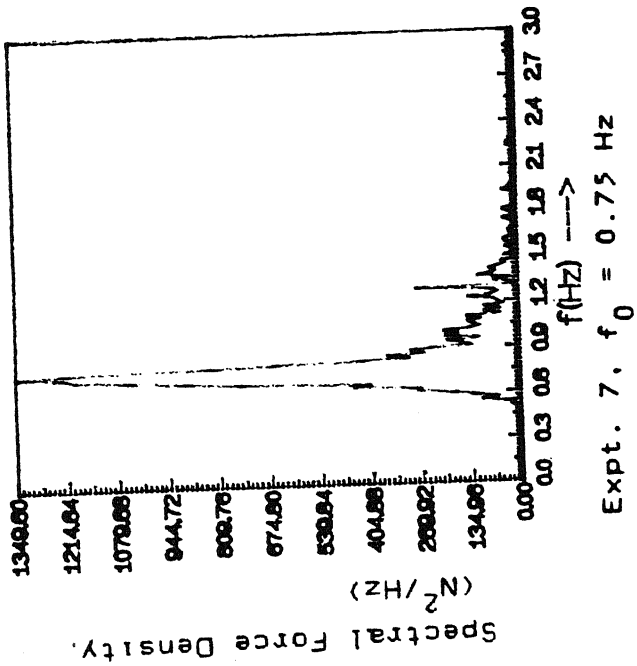

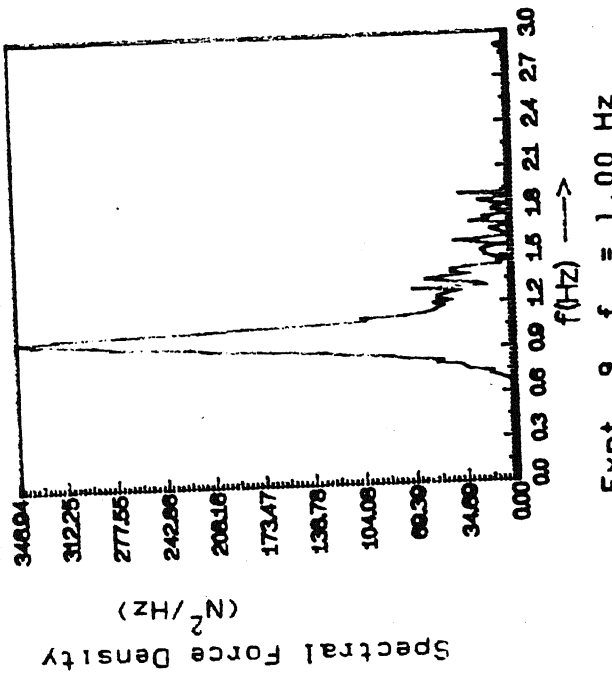

Fig. 4.6.a Lift Force Spectra for Expt. 7 to Expt. 10

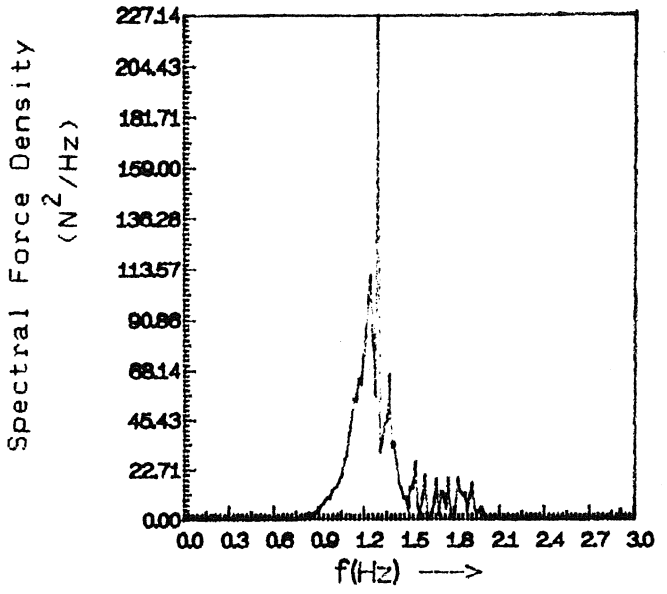

Expt. 11, f_0 = 1.25 Hz

Fig. 4.6.b Lift Force Spectra for Expt. 11

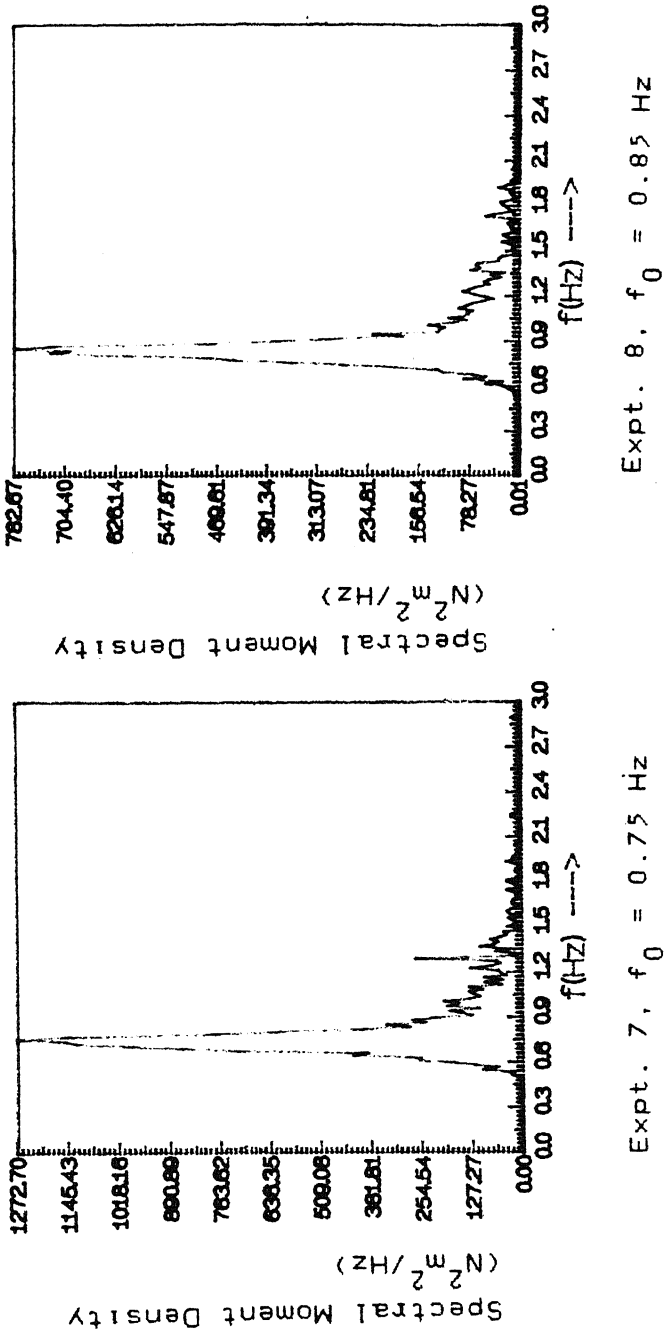

Fig. 4.7.a Lift Moment Spectra for Expt. 7 to Expt. 10

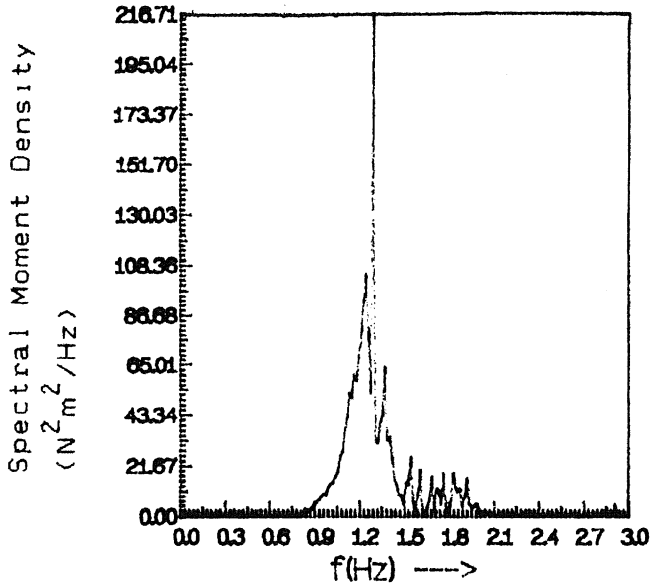

Expt. 11, f_0 = 1.25 Hz

Fig. 4.7.b Lift Moment Spectra for Expt. 11

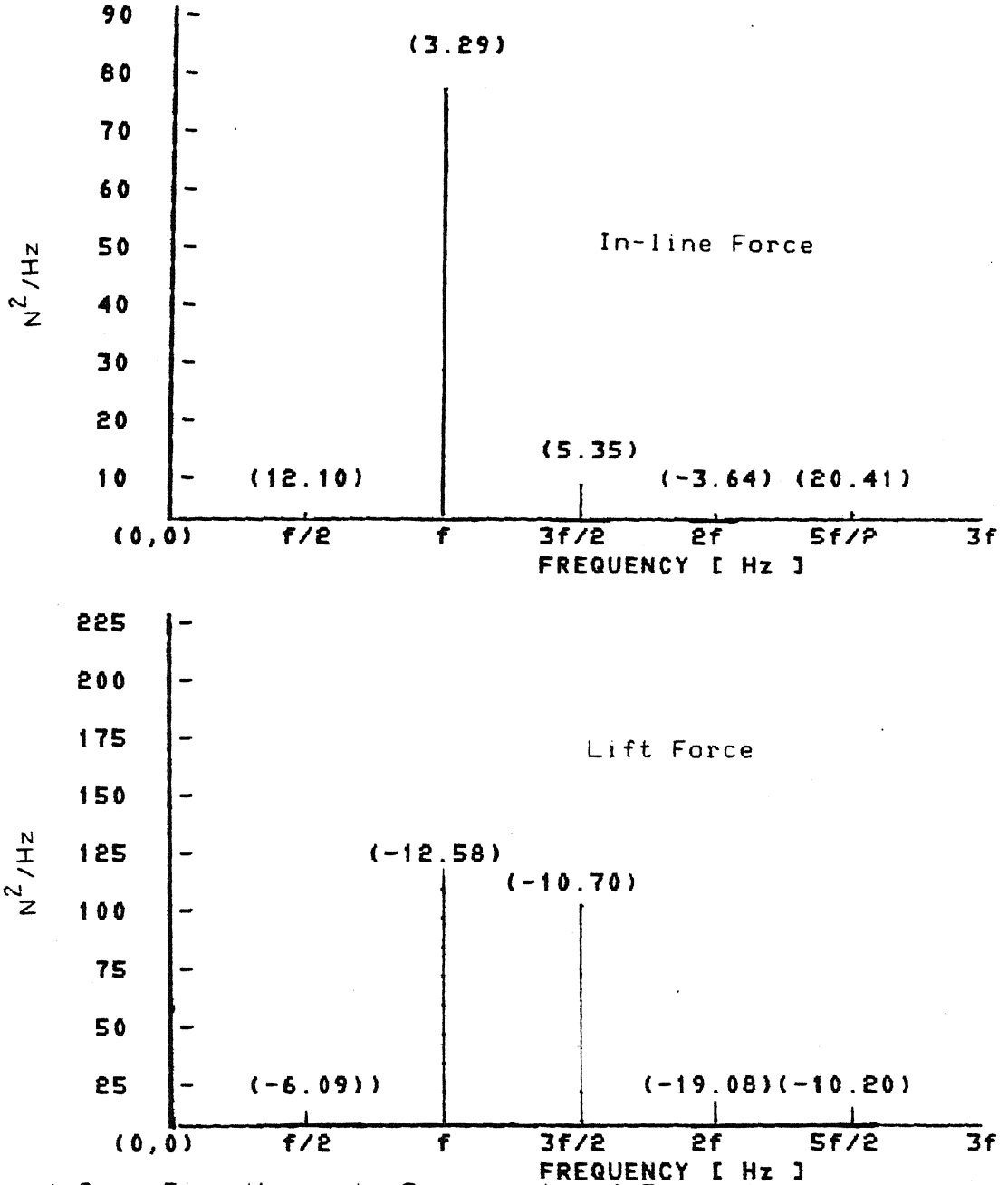

Fig. 4.8.a Five Harmonic Components of Force Spectra (Expt. 7)
f = 0.75 Hz
NOTE: NO. WITHIN BRACKETS REPRESENTS PHASE ANGLE (IN RAD.)BETWEEN WATER SURFACE ELEV. & FORCE

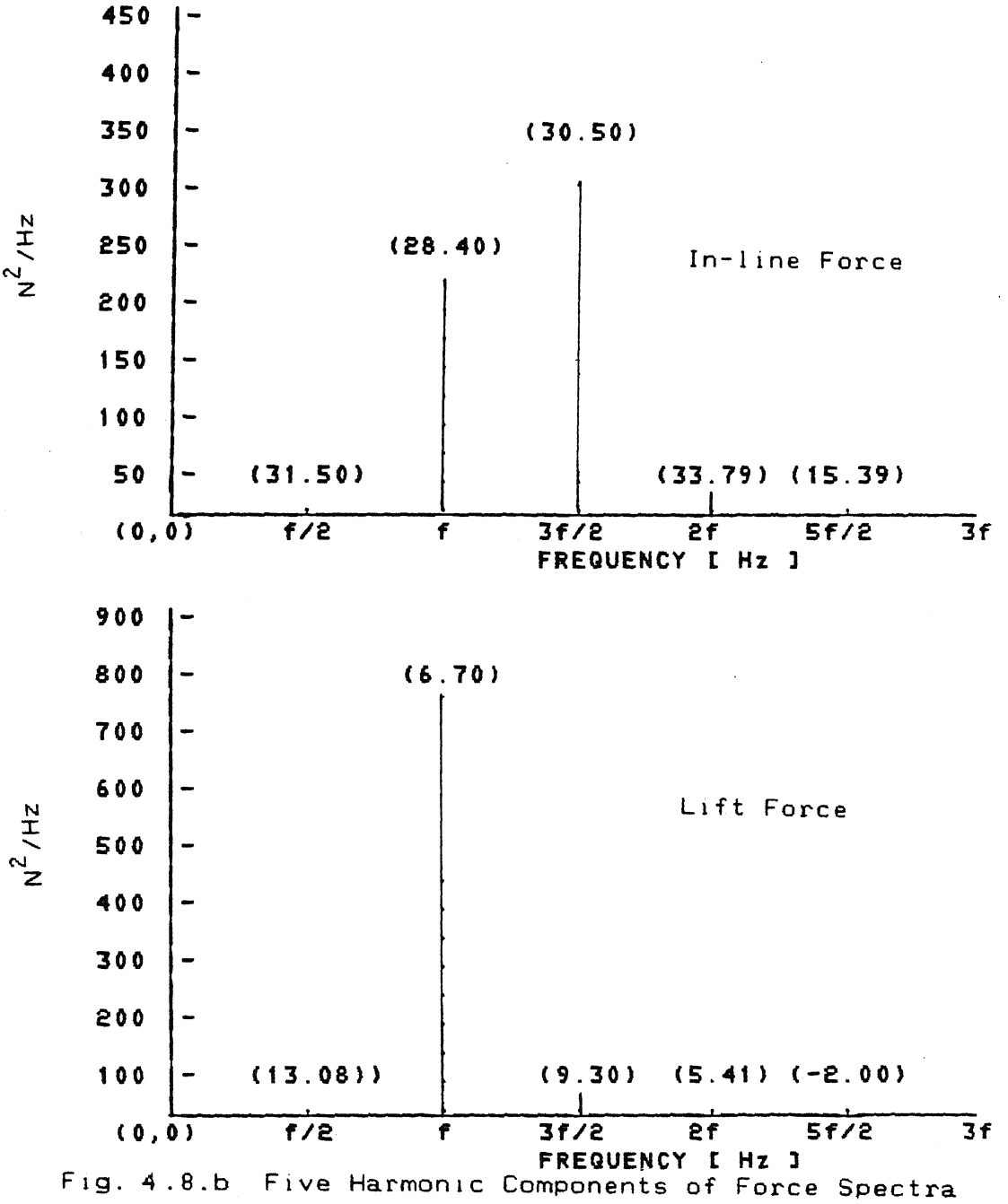

Fig. 4.8.b Five Harmonic Components of Force Spectra
f = 0.85 Hz (Expt. 8)
NOTE: NO. WITHIN BRACKETS REPRESENTS PHASE ANGLE (IN RAD.)BETWEEN WATER SURFACE ELEV. & FORCE

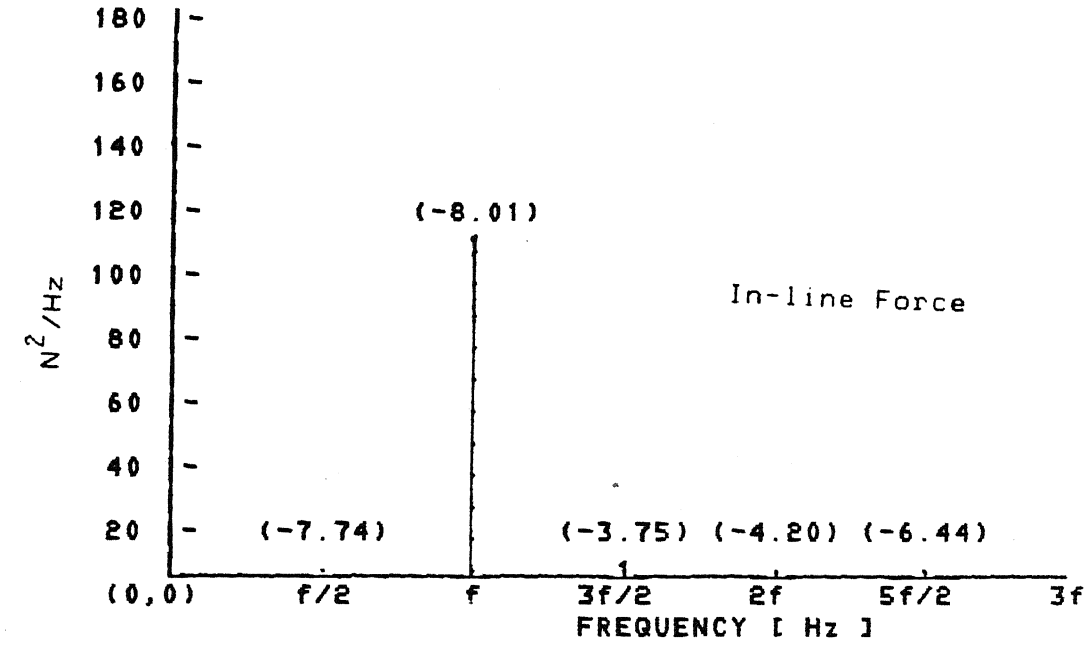

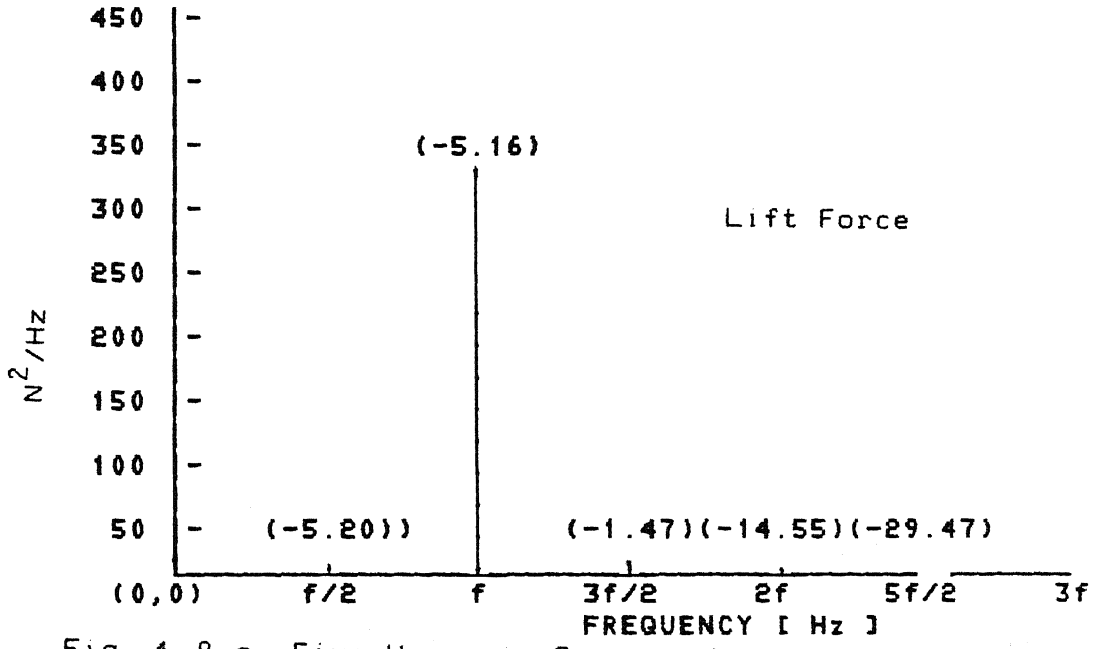

Fig. 4.8.c Five Harmonic Components of Force Spectra
f = 1.00 Hz (Expt. 9)
NOTE: NO. WITHIN BRACKETS REPRESENTS PHASE ANGLE (IN RAD.)BETWEEN WATER SURFACE ELEV. & FORCE

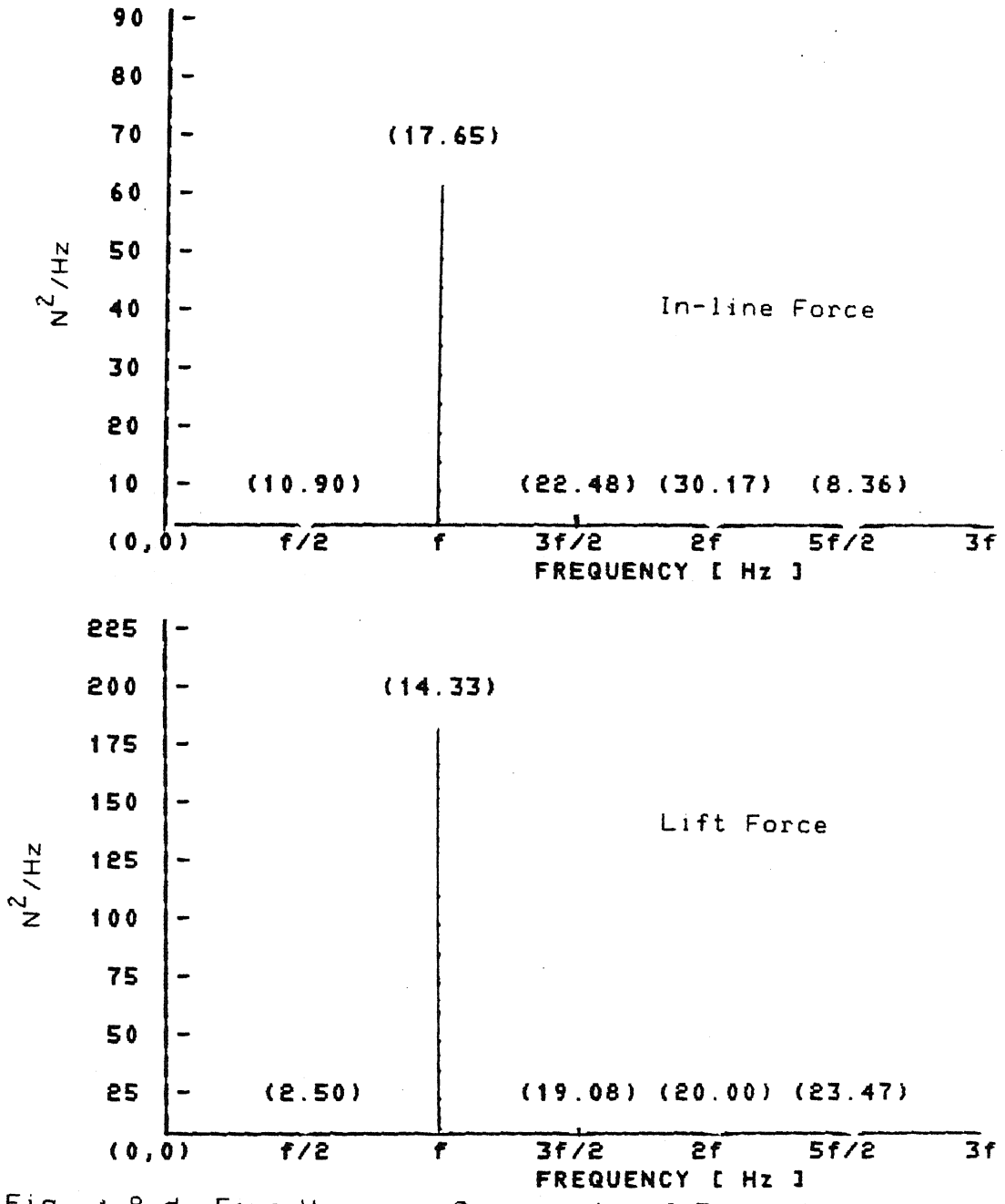

Fig. 4.8.d Five Harmonic Components of Force Spectra
f = 1.10 Hz (Expt. 10)
NOTE: NO. WITHIN BRACKETS REPRESENTS PHASE ANGLE (IN RAD.)BETWEEN WATER SURFACE ELEV. & FORCE

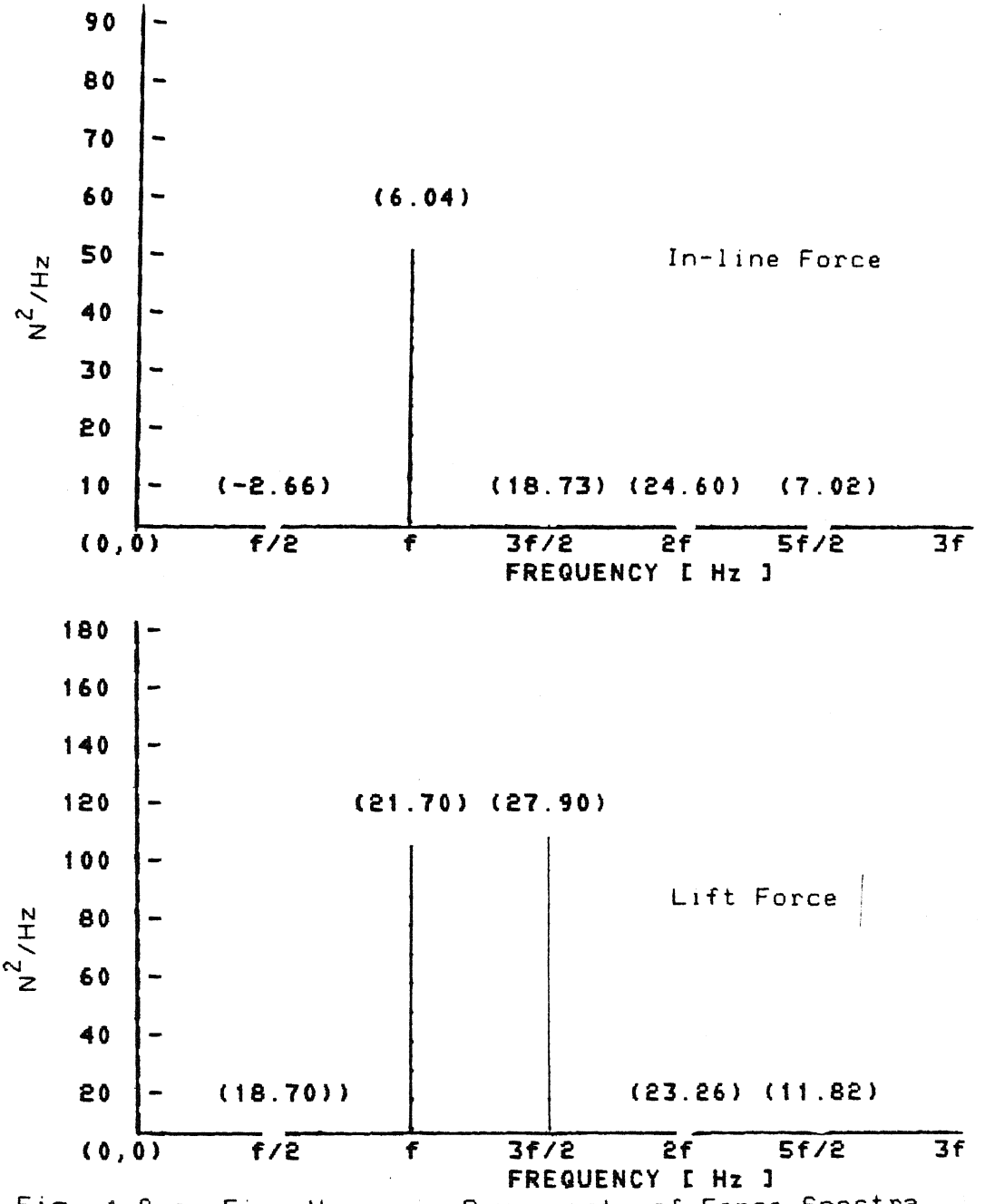

Fig. 4.8.e Five Harmonic Components of Force Spectra
f = 1.25 Hz (Expt. 11)
NOTE: NO. WITHIN BRACKETS REPRESENTS PHASE ANGLE (IN RAD.)BETWEEN WATER SURFACE ELEV. & FORCE

CHAPTER V

CONCLUSIONS

Based on the results obtained, the following conclusions have been arrived at.

(1) The maximum in-line force and maximum in-line moment increase with increasing frequency of regular waves.

(2) The maximum in-line force and maximum in-line moment increase with increasing waveheight of regular waves.

(3) The lift (transverse) force may be larger than the in-line force if the cylinder is free to move at one end. Hence in design, lift forces can not be ignored even in one dimensional flow fields.

(4) The experimental in-line force and moment spectra match with the predictions of Borgman(1967,b) at higher peak frequencies.

(5) With increasing peak frequency, water surface elevation spectrum becomes increasingly sharp, whereas the corresponding force and moment spectra remain nearly Gaussian and maintain an almost constant value of spectral width parameter ($\simeq 0.9$).

(6) In case of the random waves, the harmonic components of forces are not in phase with their corresponding water surface elevation components.

REFERENCES

1. Keulegan G.H., and Carpenter L.H., Forces on cylinders and plates in an oscillating fluid, Journal of Research, National Bureau of Standards, Vol. 60, pp. 423-441, 1958.

2. Laird, A.D.K., Water forces on flexible oscillating cylinders, Journal of Waterways and Harbors Division, ASCE, Vol. 88, No.WW3, Proc. Paper 3234, pp. 125-137, Aug., 1962.

3. Sarpkaya, T., Forces on cylinders and spheres in a sinusoidally oscillating fluid, Journal of Applied Mechanics, pp. 32-37, Mar., 1975.

4. Sarpkaya, T. and Isaacon, M., Mechanics of waveforces on offshore structures, VNR Company, 1981.

5. Shore protection mannual, Vol.II, U.S. Army Coastal Engg. Research Centre, 1977.

6. Tutor, O., Forces on cylinders and spheres in an oscillating fluid, M.S. Thesis presented to the Naval Postgraduate School, 1974.

APPENDIX - A

LISTING OF PROGRAMMES

```
      PROGRAM FFTAC
C     CALCULATION OF POWER SPECTRUM OF SIGNALS USING FFT.
      dimension a(3200),power(3200),auto(3200),alag(3200)
      dimension b(3200),a2(3200),time(3200)
      complex x(3200)
      common / tr /troom

      print *, 'what are nu ndata del'
      read *, nu,ndata,del
      scale=10.0

      n=2**nu
      tt=del*(n-1)
      pi=3.1415926

      open(unit=21,file='p',status='old')
      read(21,*) (time(i),a(i),i=1,ndata)
      close(unit=21,status='keep')

c     remove  stray mean.

      call trap(a,ndata,e)
      do 65 i=1,ndata
      a(i)=a(i)-e
65    continue

c     filter data (Tukey- Hanning formula).

      ttl=0.5*del*(ndata-1)
      do 75 i=1,ndata
      tl=del*(i-1)
      wt=1.0
      a2(i)=a(i)**2
      a(i)=a(i)*wt*scale
75    continue

      call trap(a2,ndata,variance)

      do 45 i=ndata+1,n
      a(i)=0.0
45    continue
```

```
      call fft(a,b,x,nu,del)

      do 100 i=1,n
      r=real(x(i))
      s=imag(x(i))
      power(i)=(sqrt(r**2+s**2))/tt
100   continue
      print *, 'power spectrum calculated'

      delf=1.0/tt

      open(unit=22,file='power.dat',status='unknown')
      fnyquist=1.0/(2.0*del)
      do 85 i=1,ndata
      if(b(i).ge.fnyquist) go to 86
85    continue
86    ij=i
      write (22,1130)
1130  format(/2x,'frequency in Hz; amplitude dimensionless',//)
      write(22,1100)
1100  format(5x,'frequency',11x,'amplitude',//)
      write(22,1150) (b(i),power(i),i=1,ij)
1150  format(3x,e12.5,8x,e12.5)
      write(22,1190) fnyquist
1190  format(/5x,'Nyquist frequency=',e12.5)
      close(unit=22,status='keep')

      stop
      end

      subroutine fft(a,b,x,nu,del)
      dimension  x(3200),b(3200),a(3200)
      complex x,u,w,t
      n=2**nu
      pi=3.141592653
      tt=(n-1)*del

      do 5 jj=1,n
      b(jj) = (jj-1)/tt
5     continue

      do 6 i=1,n
      x(i)=cmplx(a(i),0.0)
6     continue

      do 20 l=1,nu
      le=2**(nu+1-l)
      lel=le/2
      u=(1.,0.)
      w=cmplx(cos(pi/float(lel)),-sin(pi/float(lel)))

      do 20 j=1,lel
```

```
c       PROGRAMME TO CALCULATE WAVENUMBER & CELERITY

C       RANDOM WAVES

c       CALCULATION OF PHASE DIFFERENCE BETWEEN TWO SIGNALS.

        dimension a1(1100),a2(1100),b(1100),power1(1100),power2(1100)
        dimension a11(1100),a22(1100)
        complex x1(1100),x2(1100)
        dimension p12(1100),time(1100),pcr(1100),p11(1100),p22(1100)
        dimension ak(1100),cel(1100),phased(1100)

        pi=3.1415
        nu=10
        n=2**nu
        pi=3.1415926

        open(unit=8,file='ph.dat',status='old')
        read(8,*) (time(i),a11(i),i=1,n)
        read(8,*) (time(i),a22(i),i=1,n)
        scale=1.0
        do 20 i=1,n
        a1(i)=a11(i)*scale
        a2(i)=a22(i)*scale
  20    continue
        close(unit=8,status='keep')


        del=time(2)-time(1)
        tt=del*(n-1)

        call fft(a1,b,x1,nu,del)
        call fft(a2,b,x2,nu,del)

C       CALCULATION OF COHERENCE FUNCTION AND PHASE ANGLE.

        do 100 i=1,n/2
        r1=real(x1(i))
        s1=imag(x1(i))
        r2=real(x2(i))
        s2=imag(x2(i))
        p11(i)=atan(s1/r1)

        p22(i)=atan(s2/r2)
        if (r1.lt.0.and.s1.gt.0) p11(i)=p11(i)+ pi
        if (r1.lt.0.and.s1.lt.0) p11(i)=p11(i)+  pi
        if (r1.gt.0.and.s1.lt.0) p11(i)=p11(i)+ 2*pi
        if (r2.lt.0.and.s2.gt.0) p22(i)=p22(i)+ pi
        if (r2.lt.0.and.s2.lt.0) p22(i)=p22(i)+ pi
        if (r2.gt.0.and.s2.lt.0) p22(i)=p22(i)+ 2*pi


        t1=r1*r2+s1*s2
        t2=s1*r2-r1*s2
```

```
      pcrm=sqrt(t1**2+t2**2)
      power1(i)=sqrt(r1**2+s1**2)
      power2(i)=sqrt(r2**2+s2**2)
      pcr(i)=pcrm/(power1(i)*power2(i))
100   continue

      do 50 i=2,n/2
 25   if (p11(i).gt.p11(i-1)) go to 50
      p11(i)=p11(i)+2*pi
      go to 25
 50   continue

      do 60 i=2,n/2
 35   if (p22(i).gt.p22(i-1)) go to 60
      p22(i)=p22(i)+2*pi
      go to 35
60    continue

      do 63 i=2,n/2
      p12(i)=(p11(i)-p22(i))
63    continue

      open(unit=17,file='ax')
      write(17,555)(b(i),p12(i),i=2,n/2)
555   format(3x,f12.5,8x,f12.5,4x,f12.5)
      close (unit=17)
      stop
      end

      subroutine fft(a,b,x,nu,del)
      dimension  x(1100),b(1100),a(1100)
      complex x,u,w,t
      n=2**nu
      pi=3.141592653
      tt=(n-1)*del

      do 5 jj=1,n
      b(jj) = (jj-1)/tt
5     continue

      do 6 i=1,n
      x(i)=cmplx(a(i),0.0)
6     continue

      Do 20 l=1,nu
      le=2**(nu+1-l)
      le1=le/2
      u=(1.,0.)
      w=cmplx(cos(pi/float(le1)),-sin(pi/float(le1)))

      do 20 j=1,le1
```

```
      do 10 i=j,n,le
      ip=i+lel
      t=x(i)+x(ip)
      x(ip)=(x(i)-x(ip))*u
10    x(i)=t
20    u=u*w

      nv2=n/2
      nml=n-1
      j=1
      do 30 i=1,nml
      if(i.ge.j)go to 25
      t=x(j)
      x(j)=x(i)
      x(i)=t
25    k=nv2
35    if(k.ge.j)go to 30
      j=j-k
      k=k/2
      go to 35
30    j=j+k

      return
      end

      subroutine trap(x,n,e)
      dimension x(1100)

      fx=0.0
      do 10 i=2,n-1
      fx=fx+x(i)
10    continue

      e=(x(1)+x(n)+2.0*fx)/(2.0*(n-1))

      return
      end
```

SAMPLE SEA- PROGRAMME TO GENERATE REGULAR WAVES

```
#include <default.h>
#include <default.ttf>
#include <macros.h>

run "1.00 hz wave 0.04m" with
  OneFreq_0(1.00,0.04)
  sample "Force_Transducer 7 April 1994" on 0
  sample "Wavegauge P1 7 April 1994" on 4
end
```

```
c          Regular wave parameters      frequency = 1.0 Hz
                                        amplitude = 4.0 cm
```

SAMPLE SEA- PROGRAMME TO GENERATE RANDOM WAVES (JONSWAP SPECTRUM)

```
#include <default.h>
#include <default.ttf>
#include <macros.h>

wave w1 = jonswap(0.75,0.0081,5.0,0.07,0.09)
wave w2 = random(w1,1)

  run "Jonswap spectrum" with
  wavemaker w2 with TTF on 0
  sample "Force_Transeducer 06 sept  1994" on 0
  sample "Wavegauge (p2) 06 sept  1994" on 4
end
```

```
c          Jonswap parameters          peak frequency = 0.75 Hz
                                              alpha = 0.0081
                                              gamma = 5.0
                                            sigma a =  0.07
                                            sigma b =  0.09
```

APPENDIX B

Theoretical calculations for regular waves

Experiment 1

Given

f = 1.00 Hz

Waveheight H = 9.468 cm

Depth of water d = 70.00 cm

Dia of cylinder D = 5.00 cm

Calculate,

$$\frac{d}{gT^2} = \frac{70}{981 \times 1} = 0.071$$

$$\frac{H}{gT^2} = \frac{9.468}{981 \times 1} = 0.0097$$

Referring to the shore protection mannual, vol. II (1977)

$$\frac{L_A}{L_o} = 1.00 \quad \text{for} \quad \frac{d}{gT^2} = 0.0097 \text{ (Figure 7.44)}$$

where L_A = Wavelength in feet for period T and depth d

L_o = Deepwater wavelength ($L_o = 5.12\ T^2$) in feet

= 5.12 x 1 = 5.12

= 156.05 cm

$\therefore L_A$ = 156.05 cm.

$$\frac{D}{L_A} = \frac{5}{156.05} = k0.032 < 0.05$$

Hence, Morison equation is valid.

Now, Reynold number $Re = \frac{U_{max} D}{\nu}$

$$U_{max} = \frac{\pi H}{T} \frac{L_o}{L_A}$$

$$= \frac{\pi \times 9.468}{1} = 29.74 \text{ cm/s}$$

ν = kinematic viscosity of water at 20°C

$$= 10^{-2} \text{ cm}^2/\text{s}$$

$$\therefore \text{Re} = \frac{29.74 \times 5}{10^{-2}}$$

$$= 14872$$

Keulegan-Carpenter number

$$K' = \frac{U_{max} T}{D}$$

$$= \frac{29.74 \times 1}{5}$$

$$= 6.00$$

In order to calculate maximum in-line force and maximum in-line moment, Dean's stream function theory is being used here for Re = 14872.

$C_d = 1.2$ if $\text{Re} < 4 \times 10^4$ according to Thirrot, et al (1971).

$C_m = 2.0$ since $\text{Re} < 2.5 \times 10^5$ according to Thirrot, et al (1971).

$$W = \frac{C_m}{C_d} \cdot \frac{D}{H}$$

$$= \frac{2.0}{1.2} \times \frac{5}{9.468}$$

$$= 0.88$$

Using Dean's curves given in SPM, vol. II (1977).

for $\frac{H}{gT^2} = 0.0097$

$\frac{d}{gT^2} = 0.071$

and $W = 0.88$

We get

ϕ_m = 0.3527

α_m = 0.2564

$\therefore$ F_m = maximum In-line force

= ϕ_m w C_d H^2D (w = unit weight of water)

= 0.3527 x (1000 x 9.81) x 1.2 x (9.468×10^{-2}) x 0.05

= 1.863 N

M_m = maximum In-line moment

= α_m w C_d D H^2 d

= 0.2564 x (1000 x 9.81) x 1.2 x (5×10^{-2}) x

x (9.468×10^{-2}) x 0.7

= 0.947 Nm

Calculation of Lift force

Keulegan-Carpenter number

K' = 6.00

Using the curve for C_L given by Sarpkaya (1976a)

Lift coefficient C_L = 3.3 for Re = 14872 and K = 6.00

$\therefore$ F_{LM} = maximum lift force

= C_L . ρd D $\frac{Um^2}{2}$

= 3.3 x (100 x 0.7 x 0.05) x $\frac{(0.2974)^2}{2}$

= 5.198 N

In summary,

(a) Maximum in-line force = 1.863 N

(b) Maximum in-line moment = 0.947 Nm

(c) Maximum transverse (lift) force = 5.198 N

APPENDIX C

Some important definitions

Waveheight :

It is difference in elevation between the topmost crest and the bottommost trough of a wave over one wavelength. For a long wavetrain, waveheight is determined by averaging over individual wavelengths.

Root mean square (rms) value :

The rms value of a variable x(t) which is function of an independent variable t is mathematically defined as,

$$x_{rms} = \frac{1}{T}\int_{o}^{T} x^2(t).dt$$

where T (assumed to be large) is total t, over which we have a continuous record of x.

Spectral width parameter (ϵ) :

It is the measure of randomness of a random wave signal defined in terms of spectral moments as follows

$$\epsilon = \left[1 - \frac{m_2^2}{m_o m_4}\right]^{1/2}$$

where m_o, m_2 and m_4 are zeroth, second and fourth moments of the spectra. ϵ takes values between 0 and 1. For a narrow band spectrum $\epsilon \to 0$ (Raleigh distribution) whereas for Gaussian distribution $\epsilon \to 1.0$.

Spectral density:

The spectral density function gives the relative importance of a particular frequency component in a random wave signal. The area under the spectrum is the variance (σ^2) of the signal.

Time period:

It is the time after which a signal repeats itself.

Phase difference:

The angular separation between two harmonic waves or harmonic components of a random wave.